Nanoclay Crosslinked pH-Sensitive Hydrogel for Rhythmic Hormone Delivery

A THESIS
SUBMITTED TO THE FACULTY OF THE
UNIVERSITY OF MINNESOTA
BY

Xueyao Hu

IN PARTIAL FULFILLMENT OF THE REQUIREMENTS
FOR THE DEGREE OF
MASTER OF SCIENCE

Adviser: Ronald A. Siegel

October, 2019

Acknowledgement

I would like to express my deepest gratitude to my thesis advisor Professor Ronald Siegel, for his extensive knowledge, boundless patience, and continuous financial support. It was beyond my imagination of that such an outstanding supervisor exists. I would like to acknowledge the thesis committee member: Drs. Wang and Wiedmann, for their insightful comments, which broadened my research perspective and deepened my appreciation of science.

I would like to express my warmest sentiments to the entire Siegel research group: Siddharthya Mujumdar who had left the lab but willingly shared his experience with me via email; Davin Rautiola for always providing the help I needed in lab and in life; Krutika Jain for building the pH stat system so I could leap forward with my work only after a procedure based on this system was developed; as well as Allison Siehr, Kiki Gai, Joel Updyke, Hassaan Khan, Samuel Lee and Nicholas Langenfeld for their kind support and for sharing their projects. I must acknowledge Yizhe Zhang for trouble shooting the pH stat code issue. My sincere thanks goes to Yinong Zhao for her detailed writing instructions for my thesis, but more importantly as my best friend, doubling my joy and dividing my sorrow.

I also owe a debt of gratitude to Katie James for always handling education program matters efficiently and to Amanda Hokanson for logistical lab support and helping my student representative work all the time. I appreciate Tong Zhao, who is my friend in China, for for sharing either positive or negative emotions without restriction by jet lag. I

equally appreciate Dr. Sury's lab members for keeping a calm, positive atmosphere alive in the lab and for always being willing to help me out. Thank you also to Jiawei Wang, Yafan Su, Wei Zhang, Yuexuan Li, Jinghan Li and Zekun Shao for their company and for sharing their sweet smiles all the time.

Finally, I must dedicate this work to my parents. As a tree relies on its roots for water, nutrients and support, I too have flourished from their enriching and sustaining love and spiritual strength.

Abstract

Gonadotropin releasing hormone (GnRH) is secreted in rhythmic pulses every 1–2 hours. Disruption of this pulsatile release is associated with pathologies in reproductive function and sexual development. In order to approach an implantable, rhythmic delivery system for GnRH, a published prototype has been demonstrated that can generate rhythmic pulses of GnRH release in response to a constant glucose level. In this thesis, the prototype was altered with the intent to advance the development of a practical, implantable system. First, the commercial pH stat was replaced by a self-assembled one. The customized pH-stat was suitable for most titration conditions. Second, the durability of the membrane used in the system was improved. Third, the ratio of the membrane surface to the volume of delivery system was increased to speed up the systems oscillatory behavior. While these modifications improved the practicality of the delivery system, it resulted in the lose of pulsatile release behavior, for unknown reasons. A systematic approach is suggested, which can reveal the root cause analysis of the failure.

Table of Contents

List of Tables

List of Figures

Chapter 1 Introduction

1.1 General Introduction

Numerous endogenous hormones are known to be secreted in a pulsatile manner. For example, a neuroendocrine network controls reproduction and sexual development in mammals, where the release of hormones is not constant with time. An important reproductive hormone in human puberty and reproduction, gonadotropin releasing hormone (GnRH), is released in rhythmic pulses from the hypothalamus every 1–2 hours to stimulate secretion of luteinizing hormone (LH) and follicle stimulating hormone (FSH) in the anterior pituitary gland. GnRH subsequently degrades within a few minutes while the downstream signals carry out their actions in the human body. Disruption of this rhythm is associated with pathologies in reproductive function and sexual development. Central precocious puberty occurs when the GnRH pulse generator is initiated too early in development. Conversely, a developmental delay of GnRH release gives rise to delayed puberty [1]. Kallmann syndrome (KS) associated with anosmia, will also present if GnRH secretion is reduced [2]. KS is diagnosed in about 1 in 30,000 males and 1 in 120,000 females. Additionally, depressed GnRH secretion increases the risk of osteoporosis in both man and woman. To mitigate the pathologies associated with GnRH depression, several strategies involving GnRH release have been pursued [3-5]. Any such strategy must restore not only appropriate levels of GnRH but also their pulsatility.

1.2 Background

Several administration routes, including external controlled subcutaneous pumps [6], transdermal iontophoretic delivery [7] and intranasal sprays [8], have been investigated

for GnRH release stimulation. However, the electroporation route was only investigated at room temperature [6]. The transdermal iontophoretic route may be burdensome for the patient [7]. Intranasal administration was tested in several volunteers, but raised estrogen levels and breakthrough bleeding were reported [8].

In considering an implantable, rhythmic delivery system for GnRH, it is helpful to examine studies that addressed the pulsatile delivery of other drugs. Magnetic nanohydrogels were designed to respond to pulsed magnetic fields [9]. Ca-alginate gel beads were prepared for pulsatile dextran release. The use of various bead diameters produced different time intervals for dextran release [10]. However, only a limited number of pulses are possible with this formulation. Multi-layered capsules with biodegradable layers between drug layers were proposed, but could not be realized due to manufacturing difficulty [11].

We propose to construct a hormone release system, which can produce pulsatile drug delivery in response to endogenous stimuli, such as plasma glucose (Figure 1.1). It is noteworthy, that this system will generate rhythmic pulses of GnRH release, even though the blood glucose concentration remains constant. This is in contrast to system that deliver pulses of insulin in response to changes in blood glucose level [12].

So as to release the high potency and low dose GnRH, a previous hydrogel-enzyme based system (Figure 1.2) was achieved [13-16]. Previous publication demonstrated that under proper conditions, the system exhibits rhythmic pulsed GnRH release with internal pH.

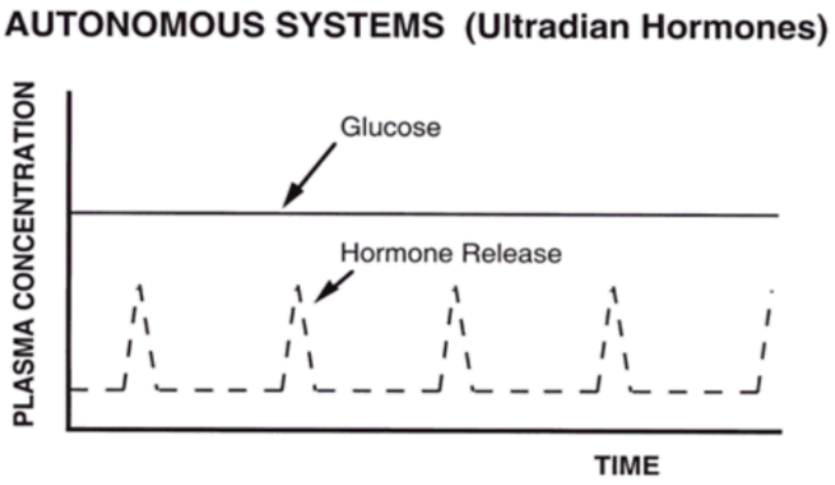

Figure 1.1 Rhythmic pulsatile GnRH release profile in the present if blood glucose level constant. [13]

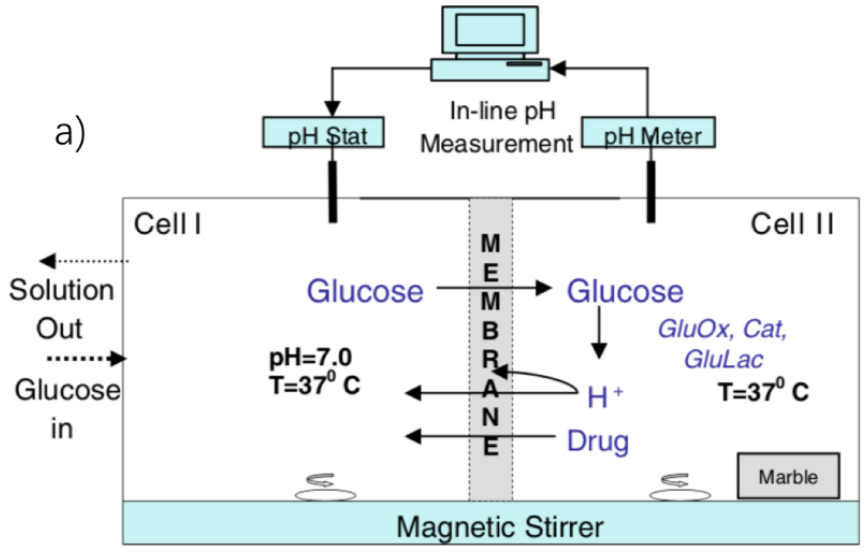

b)

$$\text{Glucose} + O_2 + H_2O \xrightarrow{GluOx} \text{Glucono lactone} + H_2O_2$$

$$\text{Glucono lactone} \xrightarrow{GluLac} \text{Gluconic Acid} \rightarrow \text{Gluconate}^- + H^+$$

$$H_2O_2 \xrightarrow{Cat} \tfrac{1}{2}O_2 + H_2O.$$

Figure 1.2 Schematic of glucose-driven drug delivery system. a) A published prototype of a glucose driven chemical pH oscillator. b) Enzymatic metabolism of glucose molecules in Cell II. [14]

Figure 1.2 a) is a schematic diagram of a benchtop prototype for a drug delivery system that is capable of releasing drug in a rhythmic, pulsatile manner. Cell I represents the circulation, which provides a steady input of glucose and allows "waste removal" from the system. Cell I is well stirred and maintained at 37 °C by a water jacketed beaker, and is also pH-controlled at 7.0. Cell I is constantly fed with an aqueous glucose solution of a specified concentration, prepared at pH 7.0, with an ionic strength of 50 mM by addition of NaCl. Cell II also contains 50 mM NaCl aqueous solution along with enzymes glucose oxidase (*GluOx*), gluconolactonase (*GluLac*), and catalase (*Cat*). Like Cell I, Cell II is well stirred and maintained at 37 °C. Finally, Cell II contains a piece of marble ($CaCO_3$). Cells I and II are separated by a hydrogel consisting of poly(N-isopropylacrylamide-*co*-methacylic acid) (NIPA/MAA), crosslinked with methylenebisacrylamide (BIS). As discussed in Chapter 3, this membrane is charged, swollen and permeable to glucose and to drug, when Cell II is at high pH, but is uncharged, collapsed and impermeable to glucose and drug with Cell II is at low pH. Cell II plus the membrane together form the prototype drug delivery system.

The proposed mechanism for the control of drug release is explained as follow. For this pulsatile, cyclic process, it can be initially assumed that the membrane is in the charged, swollen state. As such, glucose from Cell I will permeate the membrane into Cell II, where it is rapidly reacted with oxygen, due to enzyme catalysis (reaction summarized in Fig. 1.2 b). Hydrogen ion (H^+) and gluconate anion are products that cause a lowering of pH in Cell II. The hydrogen ion then diffuses into the membrane, and neutralizes the negatively charged, pendant carboxylate groups on the methacrylate polymer. Eliminating the electrostatic repulsion causes the hydrogel membrane to collapse. In the

collapsed state, the membrane blocks glucose entry, and production of H^+ is attenuated. Eventually, the hydrogen ions in the membrane diffuse into Cell I and the hydrogel ion in Cell II is neutralized by the marble, causing pH in Cell II to rise. In a time dependent manner, determined by the properties of the membrane and cell conditions, the pH in Cell II rises enough for the membrane to revert back to its swollen state, and glucose can re-enter Cell II, restarting the cycle. As the membrane goes through cycles of swelling and collapse, it alternatively permits and blocks drug release, giving rise to rhythmic, pulsatile release behavior.

The previous description is ideal, insofar as it assumes that the membrane is either permeable to glucose or is completely impermeable. In fact, even in the collapsed state, the membrane exhibits a small but nonzero permeability to glucose. Hence, the oscillatory behavior will not occur for all glucose concentrations in Cell I. Specifically, if the glucose concentration is too low, then the rate of H^+ generation in Cell II will be too slow to cause sufficient neutralization for membrane collapse, and the membrane will remain in a swollen state. On the other hand, if glucose concentration in Cell I is too high, then there will be sufficient flux of glucose into Cell II to allow continuous production of H^+ and permanent collapse of the membrane. Thus, oscillations will only occur in response to a range of glucose concentrations in Cell I.

Early experiments showed that this system, in the absence of marble in Cell II, slowly evolved to a steady state of intermediate pH in Cell II and intermediate permeability to glucose. When marble was added and glucose concentration in Cell I was increased, pH oscillations in Cell II were observed, as was rhythmic pulsed release of drug. Marble has

the effect of consuming H^+ by the reaction $2H^+ + CaCO_3 \rightarrow Ca^{2+} + CO_2 + H_2O$. This consumption amounts to increased "clearance" of H^+ from Cell II, and a higher "rate constant" for a change of H^+ concentration, i.e. pH in Cell II can change more rapidly. Such rapid pH changes appear to be necessary to prevent the membrane from relaxing into a state of intermediate permeability.

In this thesis, the goal was to convert the *in vitro* prototype, pulsatile device into a system that can be practically implanted and provide pulsatile drug delivery. There are three key aspects that were addressed. First, we sought to replace the commercial pH-stat that we used, which was purchased commercially and is quite expensive, with a home-built device. Second, a nanoclay crosslinker was evaluated as a replacement for the organic BIS crosslinker in the hydrogel membrane to achieve improved membrane durability. Third, the ratio of the membrane surface to the volume of Cell II was increased in an effort to eliminate the need for marble, which would provide an alternative means to increase the "clearance" of H^+, and hence the rate constant for change in pH in Cell II. Additionally, we wish to optimize glucose-driven oscillation concentration at body glucose level by reducing the membrane thickness to enhance glucose permeability.

1.3 Overview of the Thesis

Chapter 1, this chapter, presents a brief review of the medical problem of interest, several pharmaceutical approaches to date and a brief review of a rhythmic delivery system prototype which we hope to improve. Chapter 2 provides the working principle of a customized pH stat as well as associated experiments used in its evaluation. Chapter 3 contains the characterization of the primary material, pH-sensitive hydrogel, for the

delivery system, with an emphasis on the properties related to device performance. The integrated, new prototype delivery system is described in Chapter 4, along with evidence addressing the performance of the system. Optimization methods and future direction is summarized in Chapter 5.

Chapter 2 pH Stat

2.1 Introduction

A pH stat is a control system for maintaining the pH of a solution at a specific experimental set point. Commercially available pH stats are costly and lake the design to maintain a constant volume. As a result, we chose to construct our own pH stat with Raspberry Pi, a single board computer programmable for specialized experimental use. In order to customize the control system to our needs, we have applied several methods to adjust the machine and compared the reliability among them. The final pH stat was able to perform well during our experiments, despite some minor drawbacks.

2.2 Materials and Methods

2.2.1 pH Stat

The pH-stat programmed by Raspberry Pi (Monkmakes) consists of a probe to measure the pH of the solution and two peristaltic pumps to dose acid or base to maintain the pH of the solution at the target value. We assembled the pH stat (Figure 1.1) by fitting a RasPiRobot Board V3 (RRB3) on a Raspberry Pi computer board. The Raspberry Pi board is also connected to a power source, a monitor, a mouse, and a keyboard to enable basic commands and data output. The RRB3 is connected to a pH circuit and probe to measure pH. Peristaltic pumps are also activated by the RRB3 to make pH adjustments by pumping into or draining solution into or from the experimental environment.

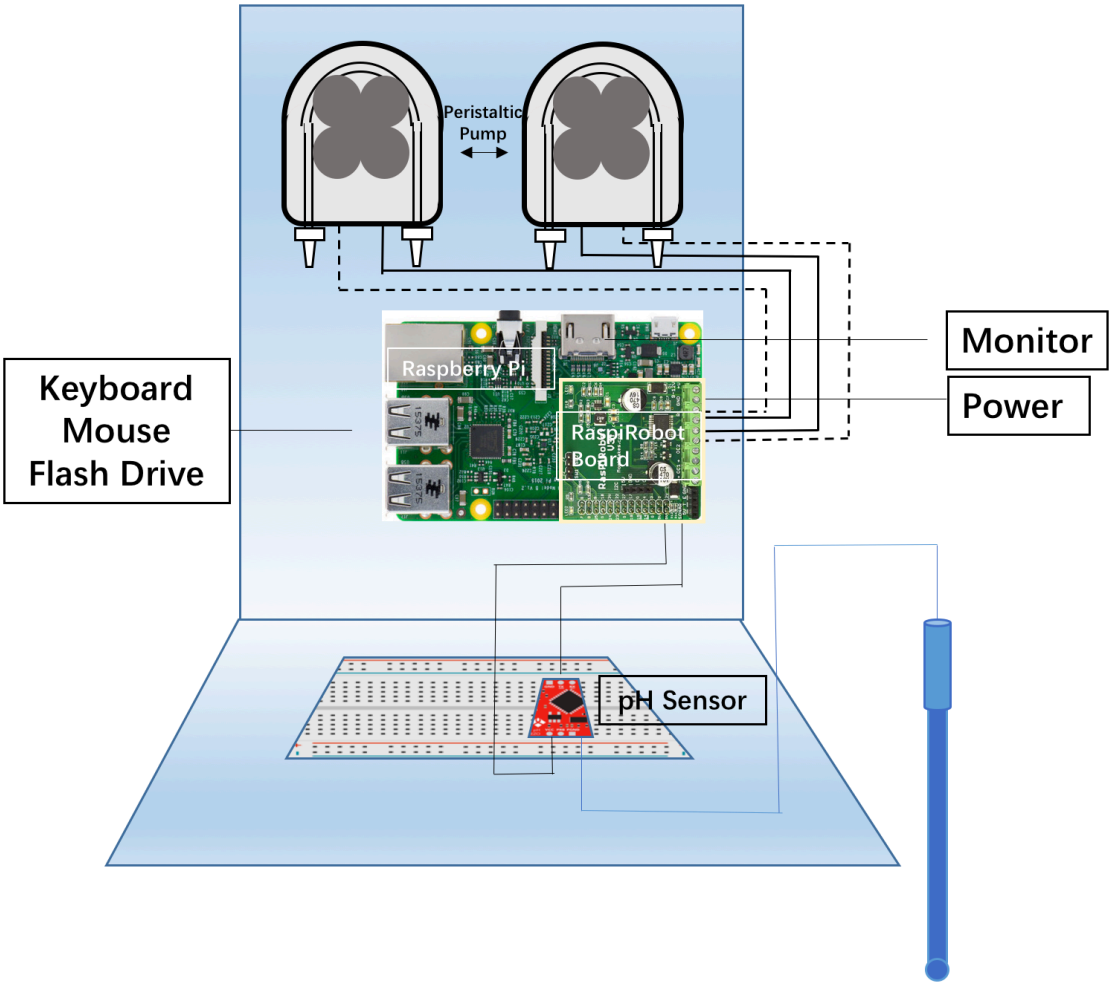

Figure 2.1 Assembly of the pH stat. Different line styles represent cables. The dashed line and solid line stand for negative and positive terminals, respectively.

Connecting cables in the reverse order cause the motors to run in the opposite direction; the directions can also be modulated by the computer code. Other external devices, such as the power source and keyboard, are displayed as text.

2.2.2 Peristaltic Pumps

The peristaltic pumps (Williamson) alternate compression and relaxation of tubing to transport the desired amount of solution into and out of the experimental environment (Figure 2.2). The motor-operated rollers pump solution through the tubing to deliver the microscale volumes that are necessary for our study. We chose a pump with four rollers

and 0.8mm diameter silicon tubing to achieve a slow enough fluid flow rate in order to deliver volumes as small as 0.05 mL/min.

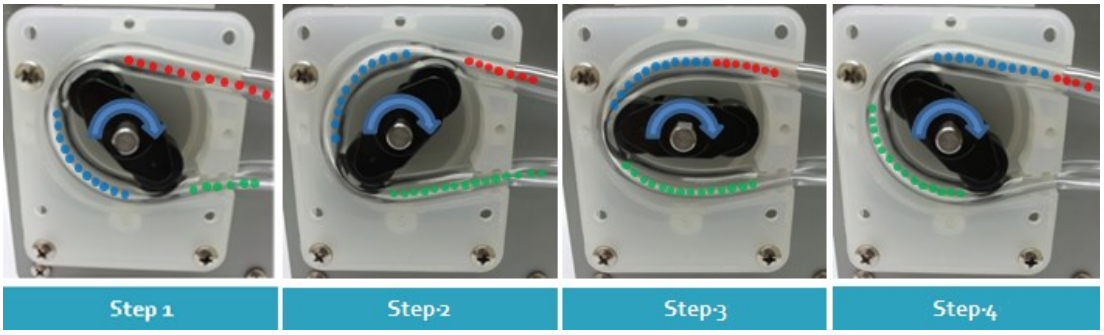

Figure 2.2 Work principle of peristaltic pump [17].

2.2.3 Raspberry Pi

Raspberry Pi (Figure 2.3) is a credit-card sized computer that works with a monitor, keyboard, and mouse to program experiments. NOOBS is the official operating system for all models of Raspberry Pi. Customization of Raspberry Pi is conducted through Python codes as shown in the following sections. NOOBS allows Wi-Fi internet connection to share experimental data with a computer.

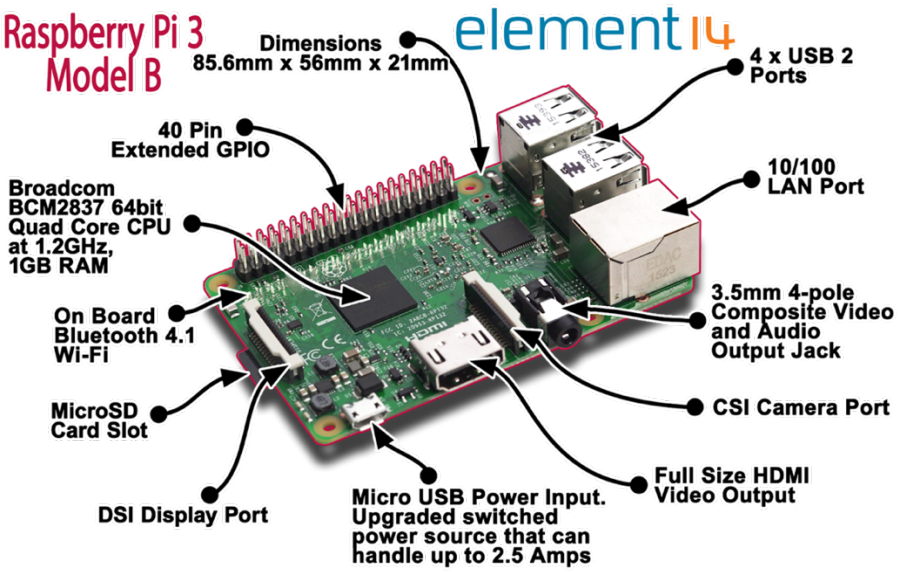

Figure 2.3 Raspberry Pi board with detailed input and output instructions [18].

2.2.4 RasPiRobot Board

The RasPiRobot board V3 (RRB3) (Figure 2.4) powers the Raspberry Pi and controls the motor function of the pH stat. The board fits right on the Raspberry Pi's GPIO socket. The RRB3 charges the motors on the peristaltic pumps to control the speed and direction of the pumping motion.

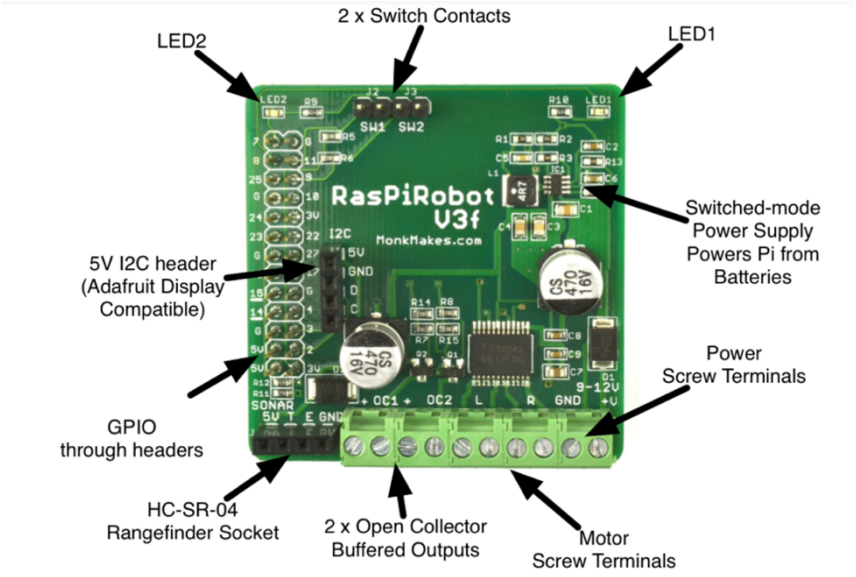

Figure 2.4 RasPiRobot board detailed part instruction [19].

2.2.5 pH Meter

The EZO pH circuit (Atlas scientific, Figure 2.5) is a pH sensor wired with RRB3 and a pH probe to read and write the pH data file. It snaps into the breadboard. The EZO pH circuit enables measurement from 0.001 to 14.000 with ± 0.002 pH unit accuracy.

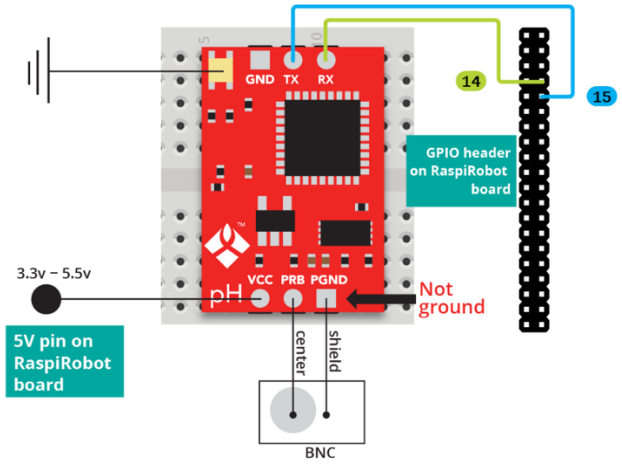

Figure 2.5 EZO pH circuit specifications [20].

A double junction, glass micro pH electrode (Thermo scientific) was connected to the EZO circuit by a BNC connector. The pH probe and EZO circuit work together as the pH meter.

2.3 Working Principle

The pH stat is controlled by several Python code packages. We used the following code packages listed below to control the pH stat. The code can be adapted to suit specific project environments and exercise better control in different projects.

2.3.1 pH Meter

The following manual commands are run in Raspberry pi terminal drive to call the pH meter and activate data input and output. Once the pH probe reads the data from the experimental solution, Raspberry Pi generates a "pH.txt" file under the installed package folder for data analysis [21].

```
Sudo python i2c1.py          #open pH meter work file
Address,99                   #tell EZO pH circuit communicate with the Raspberry Pi
Poll, "n"                    # read pH data every "n" second
Control+C                    # stop reading pH
cal,low/mid/high,"x"         #calibration pH meter with three different buffers. "x" is
```

the calibration midpoint

2.3.2 Peristaltic Pump

1. Working Principle of the Motor

The actions of the two motors in the peristaltic pump are directed by the following Python code. The motor rate is calculated for each motor as the volume extracted per unit time. The left motor runs with an arbitrary speed scale setting of 0.8 in clockwise direction, as indicated by "1". The right motor has an arbitrary speed scale setting of 0.9 in the counterclockwise direction and is indicated by "0". The actual speed of arbitrary scale was calibrated to produce desired flow rate. Despite the different motor rates, the left motor and the right motor are able to deliver the same volume per unit time, 0.5ml/min. This inconsistency is unfortunately due to the quality of the peristaltic pump.

```
#establish connection to pump with 12 voltage total, 6 each
from rrb3 import *
import time
rr = RRB3(12, 6)

#Run motors (left motor with speed 0.8 in the clockwise direction, right motor with speed 0.9 in the counterclockwise direction)
rr.set_motors(0.8,1,0.9,0)

#Stop pumping when pumping time "n" is up
time.sleep("n")
rr.stop()
```

2. pH Adjustment

For pH adjustment, step 1 involves entering all the parameters into the code. The system was initially set with a targeted pH of 7.0 and initial solution volume of 150 mL. The pH

stat attempts to correct the system pH when it is either above the upper limit of 7.1 or below the lower limit of 7.0. The pH stat is programmed with 60 seconds of wait time to allow solution mixing before taking the next reading of system pH.

When running Step 2, the pH file previously written by pH the meter will be read. Next, the "if loop" adjusts the pH when the pH is outside of the range of 7.0 to 7.1 [22]. For pH higher than 7.1, the program turns on the acid pump to supply acidic solution; the volume added is calculated by using a model to be described later. The volume of required acidic solution is translated into pumping time for the peristaltic pump with the equation of "pumping time=acid volume/ acid rate (0.5 ml/min)". The peristaltic pump will then transport the acidic solution for the calculated amount of time to adjust the system pH. Similarly, for pH lower than 7.0, the program will calculate the volume and its corresponding pumping time, and then run the alkali pump for the desired amount of time to correct the pH back to the target pH.

```
#Step 1: Call up file reader
from watchdog.observers import Observer
from watchdog.events import FileSystemEventHandler
from rrb3 import *

rr = RRB3(12, 6)
lower_lim = 7.0                 #lower pH set point
upper_lim = 7.1                 #higher pH set point
init_volofsolution = 150        #initial volume of solution
set_pH = 7.0                    #target pH of the experimental system
base_pH = 11                    #pH of base stock solution
acid_pH = 6.0                   #pH of acid stock solution
Mixing_time = 60                #waiting time in second for solution mixing

import time

#Step 2: Collect reading from the pH meter and record in log file
class MyHandler(FileSystemEventHandler):)
def on_modified(self, event):
    logfile = open("/home/pi/Raspberry-Pi-sample-code/pH","r")
    for line in logfile:
```

```
      pH = line
      pH = pH.strip()
      pH = float(pH)
    print pH
    logfile.close()
```

#Step 3: Check if the measured pH is below the lower limit

```
if pH < lower_lim:
```

#Turn on pump supplying alkali with a speed of 0.4 in the counterclockwise direction

```
    rr.set_motors(0.4,1,0,0))
```

#Print added base volume

```
    print("Alkali_vol")
    print("Alkali_time")
```

#Calculate volume needed to correct pH based on the acid-base equilibrium equation

```
    alkali_vol = init_volofsolution*((10**set_pH)-
(10**pH))/((10**pH)+(10**(set_pH+alkali_pH+pH-14)))
    alkali_rate = 0.5                          #Alkali solution supply rate
    alkali_time = alkali_vol/alkali_rate       #Calculate pumping time
    time.sleep(alkali_time)                    #Wait until pumping time is up
    rr.stop()
```

#Step 4: Check if the measured pH is above the upper limit

```
    elif pH > upper_lim:
```

#Turn on pump supplying acid

```
    rr.set_motors(0,0,0.5,0)
    print("Acid_vol")
    print("Acid_time")
    acid_vol = init_volofsolution*((10**( pH-14))+(10**(-
set_pH)))/((10**(-acid_pH))-(10**(-set_pH)))
    acid_rate = 0.5                            #Acid solution supply rate
    acid_time = acid_vol/acid_rate             #Calculate pumping time
    time.sleep(acid_time)                      #Wait until pumping time is up
    rr.stop()

 if __name__ == '__main__':
 event_handler = MyHandler()
 observer = Observer()
 observer.schedule(event_handler, path='/home/pi/Raspberry-Pi-
sample-code/', recursive=False)
 observer.start()
```

The acid or base volume, V_{acid} or V_{base} required to adjust to the target pH is calculated by the following acid-base equilibrium equation:

$$V_{acid} = \frac{V_{initial} * 10^{-(\text{set pH})} + V_{initial} * 10^{(\text{pH-14})}}{10^{-(\text{acid pH})} - 10^{-(\text{set pH})}}$$

$$V_{base} = \frac{V_{initial} * 10^{-pH} - V_{initial} * 10^{-(set\ pH)}}{10^{-setpH} + 10^{-(14-basepH)}}$$

Where $V_{initial}$ is the initial volume.

3. Modified pH Stat for the pH-Sensitive Hydrogel Project

We modified the pH stat for our experiment with the hydrogel, where the experimental system would only become more acidic over time. As a result, only the base solution is needed to adjust the system pH back to the target. Additionally, we added a draining feature to the second pump in order to maintain a constant volume in the system. This is beneficial as it is easier to calculate titration using a constant volume. More importantly, the constant volume will exert constant pressure on the hydrogel, and thus the form and release profile will not be affected by any difference in water pressure.

Step 3 and 4 were replaced by the following Python code for the purpose of the hydrogel influenced environment. When the measured pH is below the lower limit of 7.0, the program will calculate the volume and pumping time of base solution using the above acid-base equilibrium equation as mentioned above. The base solution will be pumped into the experimental system to adjust back to the target pH. Meanwhile, the pH stat generates a txt file listing of the volumes of base solution pumped each time and the duration of each pumping. Once the base solution mixes with the solution, the second pump will turn on to drain solution for the same amount of pumping time to remove excess solution from the system. The measure-and-pump cycle repeats throughout the experiment.

```
# New step 3: Check if measured pH is below the lower limit
if pH < lower_lim:
# Calculate the volume of Alkali pumped and the pumping time
```

```
    alkali_vol = init_volofsolution*((10**set_pH)-
(10**pH))/((10**pH)+(10**(set_pH+alkali_pH+pH-14)))
    alkali_time = alkali_vol/alkali_rate
    print(alkali_vol)
    print(alkali_time)
# Append pH and alkali volume data to log file
    f=open('/home/pi/Raspberry-Pi-sample-code/alkali_vol_data','a')
    f.write(repr(pH)+repr(alkali_vol)+'\n')
    f.close()
#Turn on pump supplying alkali
    rr.set_motors(0,1,0.9,1)
    time.sleep(alkali_time)
    rr.stop()
# Wait until pumping time is up
    time.sleep(Mixing_time)

# New step4: Turn on draining pump to remove excess and keep volume constant
    rr.set_motors(0.8, 1, 0, 1)
    time.sleep(alkali_time)
    rr.stop()
# If pH is greater than or equal to the lower limit, then wait mixing time
    else:(beginning of else statement, when if/then statement is
'false' then to this)
    time.sleep(Mixing_time)
```

2.3.3 Empirical Equation

The aforementioned acid-base equilibrium equation is a theoretical equation that calculates the amount of acid or base solution needed for titration. However, we discovered that the equilibrium equation was not efficient for performing titration using the Raspberry Pi pH stat under most conditions. A slow titration is problematic as it would fail to properly mimic an *in vivo*, physiologic environment that maintains a constant pH. As a result, to accelerate the titration process, it is necessary to make some adjustments to the theoretical equilibrium equation.

To obtain a new titration equation, we set up several pH points and titrated manually to obtain the exact volume needed. To be consistent with the experiment, the acidic solutions of different pH values consist of saline medium and hydrochloric acid (HCl)

stock solutions of various pHs to achieve a total volume of 150mL and final saline concentration of 50mM. The basic solution is a mixture of saline medium and sodium hydroxide (NaOH) stock solution with a pH of 11 and final saline concentration of 50mM. The empirical curve of titration gives a regression equation that fits better for the experiment (Figure 2.6). The regression equation of volume needed for titration has pH as its only independent variable.

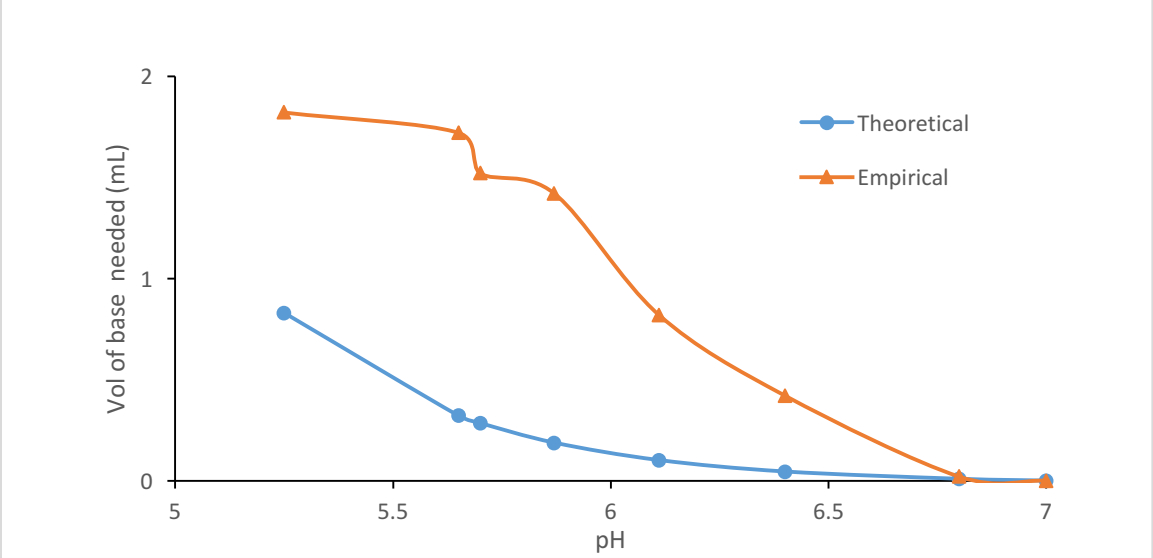

Figure 2.6 The theoretical and empirical titration curve.

1. The Polynomial Model

The following polynomial equation has the better fitted regression for the data points.

$$V_{base} = -0.4791 * pH^3 + 8.9254 * pH^2 - 56.359 * pH + 121.36$$

The R^2 for polynomial regression is 0.99534. However, the polynomial equation produces negative values when the measured pH is between 6.9 and 7. The negative value keeps the pump running and leads to overcorrection. To address this problem, we included additional code to check on the calculated pumping time. If the pumping time is

less than zero, as a result of a negative volume calculated by the polynomial equation, the code will put a stop to the pump.

```
Lower_lim = 7.0
if pH < lower_lim:
    alkali_vol = -0.4791*(pH**3)+8.9254*(pH**2)-56.359*pH+121.36
    alkali_time = alkali_vol/alkali_rate
# check if the calculated pumping time is negative
      if alkali_time < 0:
      alkali_time=0
      else:
      alkali_time=alkali_time
```

This manual fix, however, means that the pump stops running even when the experimental pH is between 6.9 and 7, lower than the target 7. Therefore, the polynomial equation fails to correct the experimental pH back to 7, the target pH.

2. The Exponential Model

Given the significant drawbacks of the acid-base equilibrium equation and the polynomial equation, we plotted the data points using an exponential regression and obtained

$$V_{base} = 5767.3 * e^{-1.546*pH}$$

This equation will always produce a positive calculated volume for titration, which solves the problem of the polynomial model. This enables the pH stat to titrate with precision even when the system pH dips slightly below 7.

It is worth mentioning that the exponential model does not perfectly align with the data points, especially when pH is lower than 5, which contributed to a lower R squared value. However, this is not a major concern, since during our experiment the pH never drops below 6. Additionally, we adjusted the Python code to apply a lower limit of 6.9, instead

of the original 7.0. The pH stat will stop titration as soon as the reading of experimental pH reached 6.9. This adjustment is unique to the exponential model to prevent overshoot. The exponential model returns a higher volume of solution needed for titration in comparison to the other equations. This can be particular problematic for small pH adjustments as low as 0.1 from the target. This is unfortunately an inherent downside of the exponential equation. To avoid overshooting, we found that setting the lower limit at 6.9 reduces unnecessary pH fluctuation while achieving the target pH.

```
lower_limit=6.9
Import math

if pH < lower_lim:
    a = math.exp(0-(1.546*pH))
    alkali_vol = 5767.3*a
    alkali_time = alkali_vol/alkali_rate
    print(alkali_vol)
    print(alkali_time)
```

2.4 Results

To test and compare the efficacy and efficiency among the acid-base equilibrium equation, the polynomial model, and the exponential model, we recorded the system pHs and time stamps using the Raspberry Pi pH stat for each model (Figure 2.7). Each measurement started with a solution of pH 5.65 (50mM saline and HCl). Then, the pH stat added a neutralizing solution of pH 11 (50mM saline and NaOH) to titrate the system pH to the targeted 7.0. The three equations were applied to each set up. The pH readings from the three models are compiled for comparison.

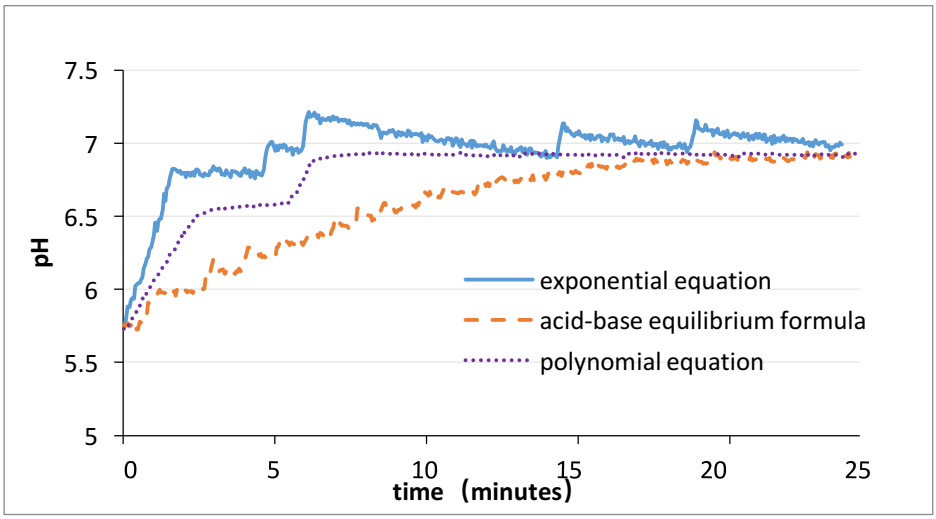

Figure 2.7 Comparison of three titration models, acid-base equilibrium equation, polynomial equation, and exponential equation.

As shown in Figure 2.7, the exponential model is the first and only one to reach target pH of 7.0 in approximately 5 minutes. The pH of the system overshoots to around 7.2 and slowly returns back to 7.0 at 12 minutes. The polynomial model takes 10 minutes, twice as long, to reach pH 6.9. It cannot achieve pH 7.0 due to the "manual stop" on the pump for pH values between 6.9 and 7.0. The limitations on speed and lower than target pH make the polynomial model unsuitable for the pH stat. Lastly, the equilibrium equation reaches approximately pH 6.8 in 20 minutes when the recording terminates. Due to the slow pH adjustment, the equilibrium equation was also deemed unsuitable to code the pH stat.

To test the responsiveness and stability of the pH stat using the exponential model, we introduced a low pH solution into the experimental solution and recorded the pH every 30 seconds (Figure 2.8). The initial titration started with a 50mM saline solution of pH 5.7. In approximately 5 minutes, the experimental pH achieved the target pH 7. Between 5 and 25 minutes, the measured pH fluctuated around 7. The pH stat was also able to raise

the pH back to 7 within 10 minutes when HCl was randomly added into the experimental system at 25,40, 50 and 62 minutes.

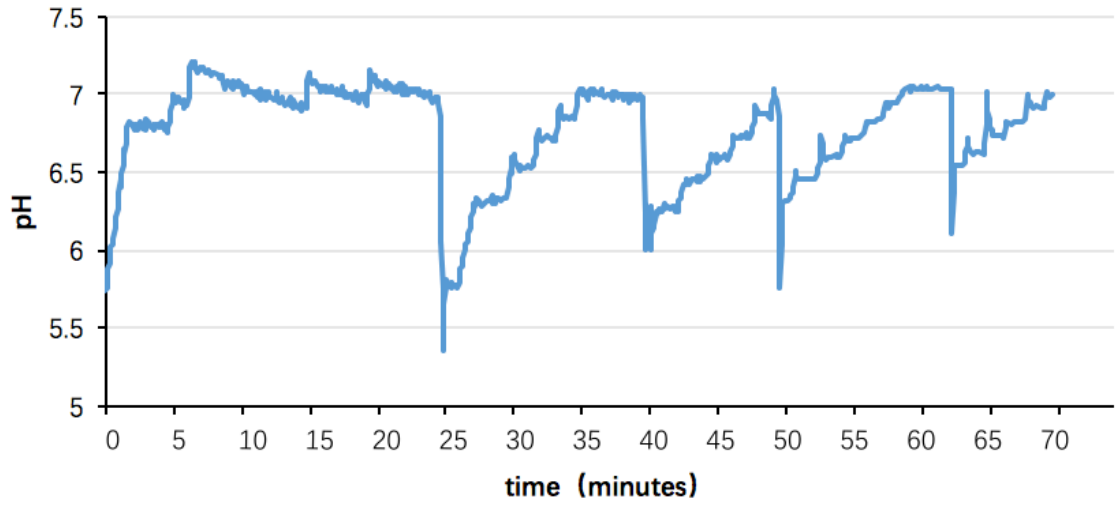

Figure 2.8 Titration recovery stability test. The pH stat is programed with the exponential equation to perform titration. The system pH is plotted against time.

The pH readings also revealed when the experimental solution was drained by the peristaltic pump. The plateaus at 3 to 5 minutes and 27 to 30 minutes represent paused titration when the solution mixes in the experimental system and the peristaltic pump drains the excess solution in the system to maintain relatively constant volume. The draining process might appear to slow down the titration because the pump delivering basic solution is programmed to pause. It is plausible to have both draining and delivery pumps work simultaneously to speed up the titration. However, the measured pH might not be accurate when the reading is taken with incomplete mixing. Therefore, it might be counterproductive to pump out nonhomogeneous solution mixture while basic solution is being added into the experimental system.

During the experiments with the hydrogel to be described in subsequent chapters , the donor chamber constantly releases hydrogen ions into the saline medium through the hydrogel, resulting in an increasingly acidic solution. To test the feasibility of applying the pH stat with the exponential model to maintain the pH under the real experimental environment, we set up a system that introduced buffers of various pH into the saline medium to create increasing acidity. The donor side was a small chamber filled with 3ml buffers of pH 3, 4, 5 and 6 that donated hydrogen ions into the rest of the system. The receptor side, containing 150ml of 50mM the saline medium, was regulated by the pH stat to maintain a pH of 7. The lower pH limit was set at 6.95 to avoid overshoot; the upper limit was set at 7.

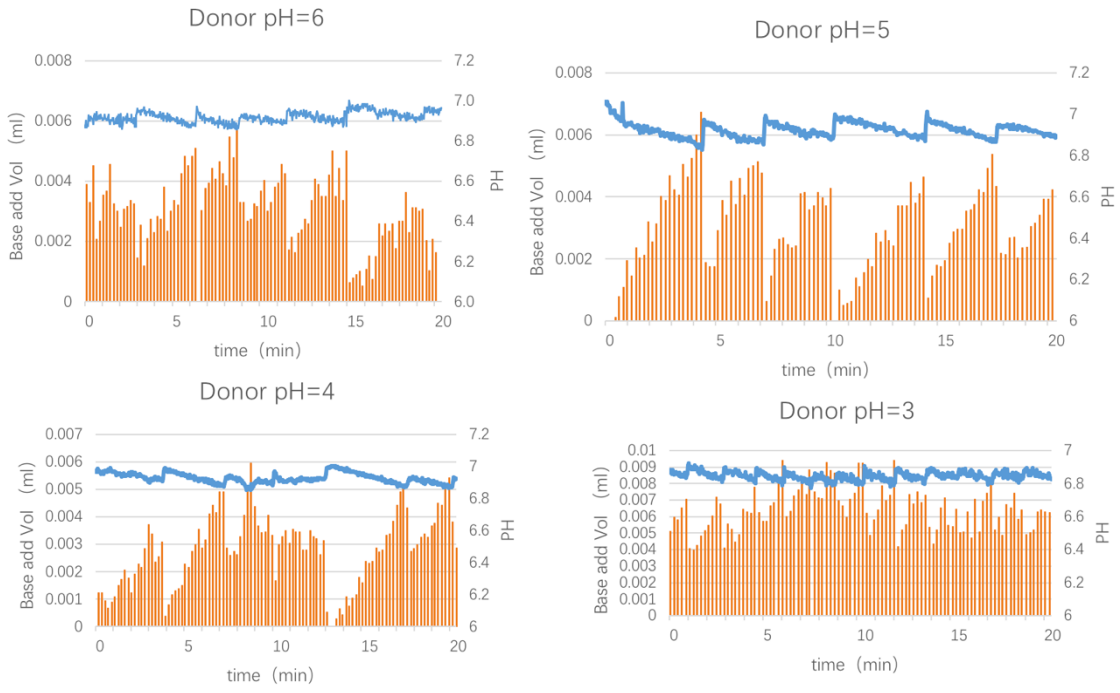

Figure 2.9 pH stability control tests. The pH stat is programmed with the experimental equation to neutralize four systems of hydrogen ion donors of pH 3, 4, 5 and 6. The system pH (blue line) and calculated volume of base solution (orange column) are plotted against time.

The pH stat successfully maintained the pH of solution to the targeted 6.95 to 7 range (Figure 2.9), with minimal fluctuation, when the donor solution's pH was between 4 and 6. When the donor side was more acidic (pH = 3), the pH stat was only able to maintain the pH between 6.8 to 6.9. The pH stat also recorded the small volumes, less than 0.01ml of base solution, added to correct the experimental pH.

2.5 Discussion

2.5.1 Evaluation of the pH Stat

The components of the pH stat were inexpensive to acquire and easy to assemble and control. While commercially available pH controllers require less setup, the higher price may not justify their convenience. The pH controller introduced here can be adapted to most titration setups with calculation and hardware adjustment. The size of the pH controller we made is much smaller than that of the commercial product.

The peristaltic pumps are suitable for accurate dosing applications. They are also adaptable to any volume or speed of solution for specific projects with different tubing and speed. The small pump size enables the pump to be secured on the same 7*6 inch circuit board as the Raspberry Pi.

The high customizability of the pH stat also contributes to its drawback, the need for empirical modification for efficient performance. The following section addressed the empirical equations and modifications of the Python code. The delivery of smaller volumes can be challenging mainly due to the surface tension of the liquid and the tube diameter, which prevents drop detachment. Thus, in some cases, the small volumes are "saved" until the next triggered released into the system. Similar to other devices, the pH

stat requires regular calibration and monitoring. Additionally, because of its homemade nature, the pH stat has an unknown lifetime.

2.5.2 Evaluation of the Empirical Equations

The constants in the empirical equations, the polynomial equation and the exponential equation, were derived from experimental data to set up the pH stat. Both equations have the advantage of achieving faster titration than the acid-base equilibrium equation that is typically used in pH control systems.

Interestingly, the titration data shows higher volume needed to achieve target pH than the theoretical volume calculated by the equilibrium equation. We suspect that this observation may have resulted from the titrated solution being in contact with air and the stirring. That is, the experimental setting allowed carbon dioxide from the air to dissolve in the solution, which converted to hydrogen carbonate and thus was also subject to titration.

Table 2.1 Comparison of the three models for titration.

Characteristics	**Base-acid equilibrium equation**	**Polynomial equation**	**Exponential equation**
Time to reach target	Long	Medium	Short
Accuracy	Exact	Lower	Exact
Overshoot	No	No	Yes
Application	Applicable to any system with some changes in parameters	System specific	System specific

Chapter 3 pH sensitive hydrogel

3.1 Introduction

Hydrogels are three-dimensional cross-linked networks with hydrophilic properties. Since Wichterle and Lim's pioneering work on poly (2-hydroxyethyl methacrylate) (PHEMA) in 1960 [23], hydrogels have sparked interest in biomedical applications and drug delivery. Taking advantage of the high water content, softness, biocompatibility, and swelling-shrinking properties, numerous researchers have investigated hydrogels for biomedical and pharmaceutical applications, including tissue engineering [24], molecular imprinting [25], wound dressing [26], immunizations [27], and drug delivery [28,29].

Responsive hydrogels have remarkable advantages for controlled release because their volumes can change predictably in response to a variety of physical and chemical stimuli. Physical stimuli include temperature, electric or magnetic field, light, pressure, and sound, while chemical stimuli include pH, solvent composition, ionic strength, and specific molecular species such as glucose [28]. Because tissues and pathological conditions vary in physiological pH, pH-responsive polymeric materials have been studied extensively for site- and disease-specific drug delivery applications [29,30]. pH-sensitive hydrogels can be categorized as anionic and cationic. Anionic or acidic hydrogels contain acidic side chains that become ionized, when the pH of the external swelling medium exceeds the pKa of the side chain [31]. Conversely, the amino side chains of cationic or basic hydrogels become ionized [32] when the external pH is lower than pKa of the side chain. Both types of pH-sensitive hydrogel can be useful for drug delivery under specific circumstances.

For this project, we will focus on acidic side chain hydrogels, which also contain the neutral comonomer, *N*-isopropylacrylamide (NIPA). NIPA is hydrophilic below 32 degrees Celsius (^{o}C). At 32 ^{o}C, the lower critical solution temperature (LCST), the hydrogel transitions from a hydrophilic to a hydrophobic entity [33]. Therefore, at physiological temperature (37 ^{o}C), NIPA will exhibit hydrophobicity. In order to explain this phenomenon, several scientists have used calorimetry to shown that the phase transition is governed by cooperative dehydration of poly(NIPA) chains [34]. Recently dielectric relaxation has been used to analyze the relaxation frequency [35]. The phase transition was associated with the complete dehydration of poly(NIPA) chains and the consequent generation of bare polymer chains at the LCST. The dielectric relaxation technique further revealed 11 water molecules per poly(NIPA), which strongly supported they hydrogen bond theory (figure 3.1). This transition is manifested in the discrete changes that occur in the mechanical, permeability and optical properties of poly(NIPA) hydrogels.

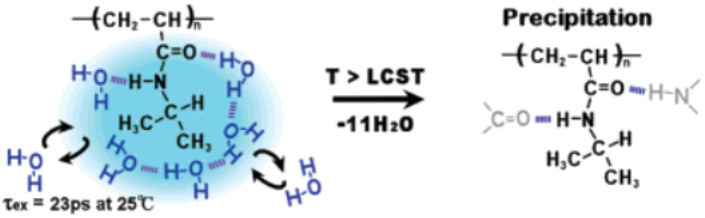

Figure 3.1 Phase transition of poly(NIPA) at LCST [35].

Methacrylic acid (MAA) is a carboxylic acid which, when copolymerized with NIPA (Figure 3.2), endows the hydrogel with pH sensitive properties. The poly(NIPA-co-MAA) hydrogel network has both pH and temperature sensitive characteristics [33]. Similarly, poly(NIPA-co-MAA) is expected to have an LCST where the phase transition

takes place by breaking hydrogen bonds and losing water molecules. The side chains of poly(NIPA-co-MAA) further affects the LCST under different pH values due to the changes in their hydrophilicity.

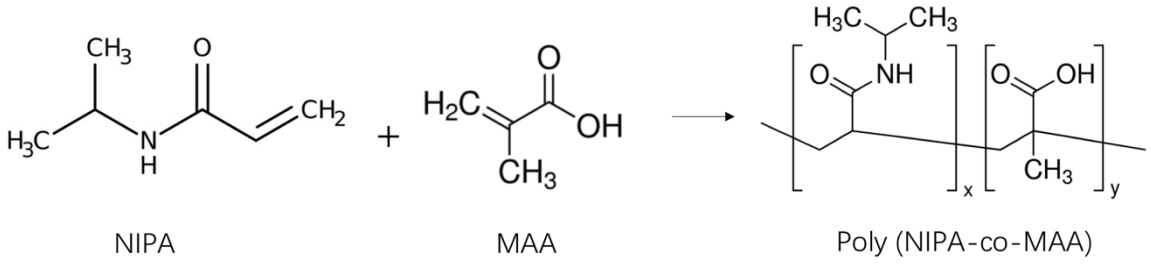

Figure 3.2 Chemical structure of Poly (NIPA-co-MAA).

According to a previous study [36], a 9:1 molecular ratio of the NIPA and MAA monomers produces hydrogels with a large linear swelling ratio (Figure3.3).

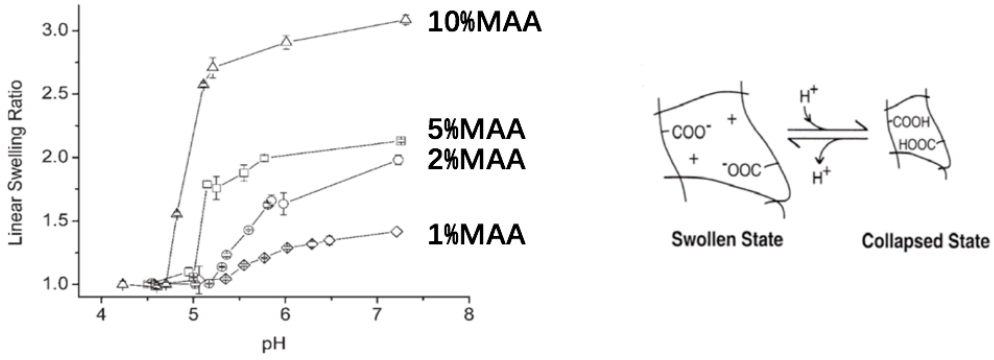

Figure 3.3 pH-dependent equilibrium swelling studies at 37 ^{o}C, swelling transition magnitude and critical pH depends on MAA content [36, 37].

However, increasing the percentage of MAA molecules during the synthesis reduces the mechanical strength of the hydrogel [37]. Since the swelling ration is considered one of

the most important property, the 9:1 NIPA to MAA ratio was chosen to create the polymer for a pulsatile drug delivery system.

In order to increase the mechanical strength of the hydrogels, we introduce nanoclay as crosslinker. Laponite XLG (diameter 25nm and thickness 0.92nm) consists of negatively charged silicate nano-discs with slightly positively charged edges. The lamellar sheet structure, when dispersed in water, swells into a house-of-cards structure by stacking on top each other due to the opposite charge on the surfaces and edges (Figure 3.4 A).

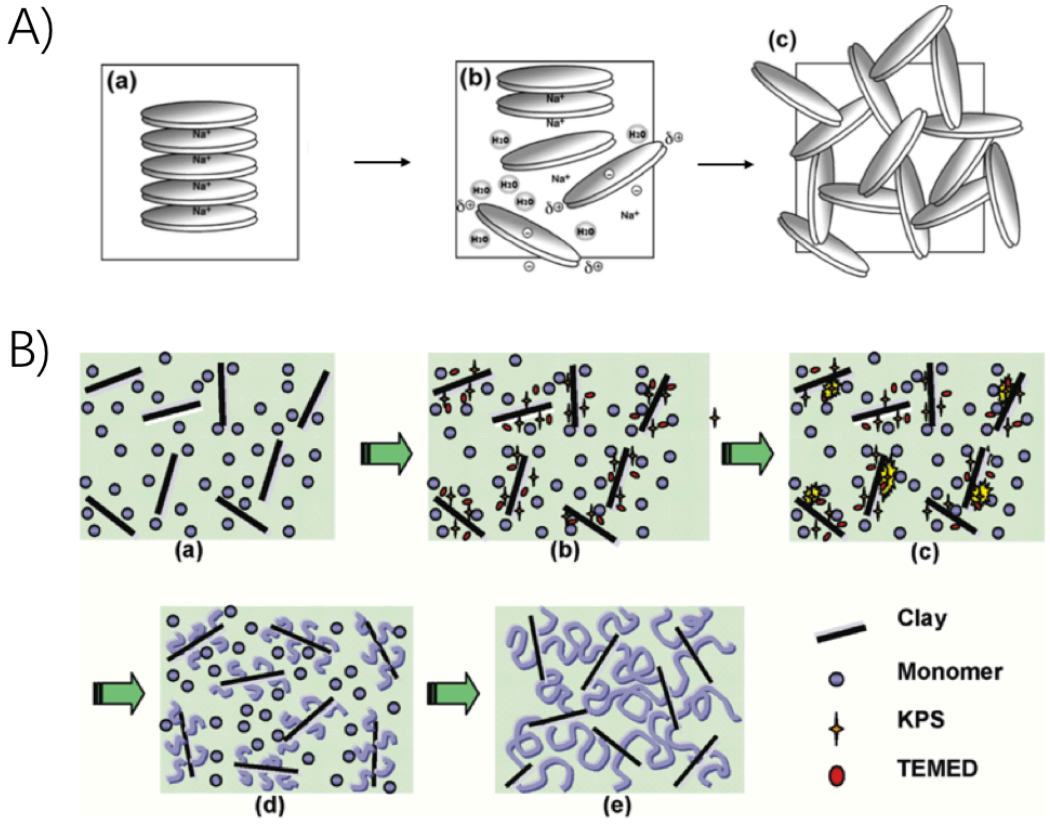

Figure 3.4 Schematic of nanoclay crosslinked poly(NIPA-co-MAA) synthesis. A) Schematic of laponite XLG nanoclay suspension and the house-of-cards structure: (a) clay, (b) clay platelets dispersed in water, and (c) house-of-cards structure. B) Schematic of Poly (NIPA-co-MAA) synthesis.The blue circles represent MAA and NIPA for synthesis in (a)-(e). (a) shows house-of-card structure has been decomposed after NIPA

comes in. (b) illustrates KPS and TEMED complexed with clay discs after added in. (c) shows radical formation near the clay surface (d) exhibits formation of clay-brush particles. (e) polymer network formation [38].

In previous work, our laboratory has utilized poly(NIPA-co-MAA) hydrogels that were crosslinked with BIS. These organically crosslinked hydrogels are mechanically weak. In the past two decades, it has been shown that NIPA containing hydrogel can be strengthened by using exfoliated laponite clay as a crosslinker [36]. Such hydrogels also exhibited superior optical and phase transition properties [39,40]. In the present chapter, we investigated the permeability properties of laponite crosslinked hydrogels.

3.2 Materials and Methods

3.2.1 Materials

NIPA (monomer; Sigma-Aldrich) was recrystallized from hexane under vacuum at room temperature. MAA (monomer; Sigma-Aldrich) was purified by passing though activated alumina (Sigma-Aldrich) to remove inhibitor. The molar feed ratio of the comonomers was 9:1 NIPA/MAA. Laponite XLG (nanoclay cross-linker, Rockwood), N,N,N',N'-tetramethylethylenediamine (TEMED, accelerator: Sigma-Aldrich), sodium pyrophosphate decahydrate (SPP, ionic dispersant: Sigma-Aldrich) and potassium persulfate (KPS, initiator: Sigma-Aldrich), were used as received. The deionized (DI) water was ultrasonically degassed, and the gas bubbles were removed by vacuum. The degassed water was used to synthesize the hydrogel. Chlorotrimethylsilane (Sigma-Aldrich) was used for silanizing glassware. Acetate buffer (pH=3.5-5.5) and phosphate buffer (pH=6-8) were prepared to cover the entire range of swelling studies. Paracetamol (Sigma-Aldrich), caffeine (Sigma-Aldrich) and Lissamine Green B (LGB, dye; Sigma-Aldrich) were used as solutes in the permeability experiments.

3.2.2 Copolymerization of NIPA with Comonomers

The anionic copolymer hydrogel, poly(NIPA-co-MAA), was synthesized using redox initiated free radical polymerization of NIPA and MAA at 5^{o}C for 24 hours. All reagents and respective quantities are listed in Table 3.1.

Table 3.1 Copolymerization of NIPA with MAA.

materials	MW (g/mol)	Amount (μl)	Amount (g)	Molar ratio	Amount (mmol)
N-isopropylacrylamide(NIPA)	113.16		0.2	90	1.767×10^{-3}
Sodium pyrophosphate decahydrate (SPP)	446.07		0.075		1.68×10^{-4}
Methacrylic acid(MAA)	86.6	17	0.017	10	1.96×10^{-4}
Clay(x-linker)			0.088		
Potassium persulfate (20mg/ml)		675	0.0135		
Tetramethylenediamine(TEMED)	116.20	5			
DI water (degassed)			2.13		

The Laponite clay was dispersed under stirring in pre-degassed deionized water to form an exfoliated and uniform dispersion of clay, which is a clear sol. Previously recrystallized NIPA monomers were then added. SPP was dissolved to prevent clay particle flocculation prior to adding MAA [36]. The reaction vessel was placed under inert nitrogen to exclude oxygen. MAA solution was then added dropwise into the mixture. Initiator, KPS, and catalyst, TEMED, were added together under bubbling nitrogen. To form the hydrogel with a membrane shape, the final mixture was injected between silanized glass plates separated by 100 μm gaskets. Solution polymerization took place at under 5^{o}C for 24 hours. Thereafter, the gel was incubated in deionized water

to remove unreacted monomer. Lastly, the finished hydrogel was placed in saline conditioning medium.

3.2.3 Equilibrium Swelling Studies

In the pH-dependent equilibrium swelling studies, poly(NIPA-co-MAA) disks were equilibrated in several pH buffers at 37^{o}C. Disk diameters were measured by a Vernier caliper over 60 minutes under different pH environments. The linear swelling ratio (LSR) was calculated by equilibrium swelling diameter at a given pH divided by 1.5cm which is the initial diameter of hydrogel. Swelling measurements were repeated three times and reported with error bars representing the standard deviation.

In the shrink ratio studies, hydrogel equilibrated in pH 7 buffer at 37^{o}C several hours before exposure to different pH buffers. In the swell ratio studies, hydrogel equilibrated in various pH buffers at 37^{o}C several hours before exposure to pH 7 buffer. The hydrogel diameters were checked at 2, 5, 7, 10, 12, 15, 20, 30 and 60 minutes.

3.2.4 Mechanical Properties

Tensile moduli and strength of hydrogels were measured using a tensile tester (MTS Criterion Model 42). Hydrogel samples were first prepared in strips of 5cm x 1cm x 100μm and stored in buffer at 37^{o}C for an hour. Tensile measurements were performed at 25^{o}C with gauge length of 15mm and crosshead speed of 100mm/min.

3.2.5 Drug Permeability Studies

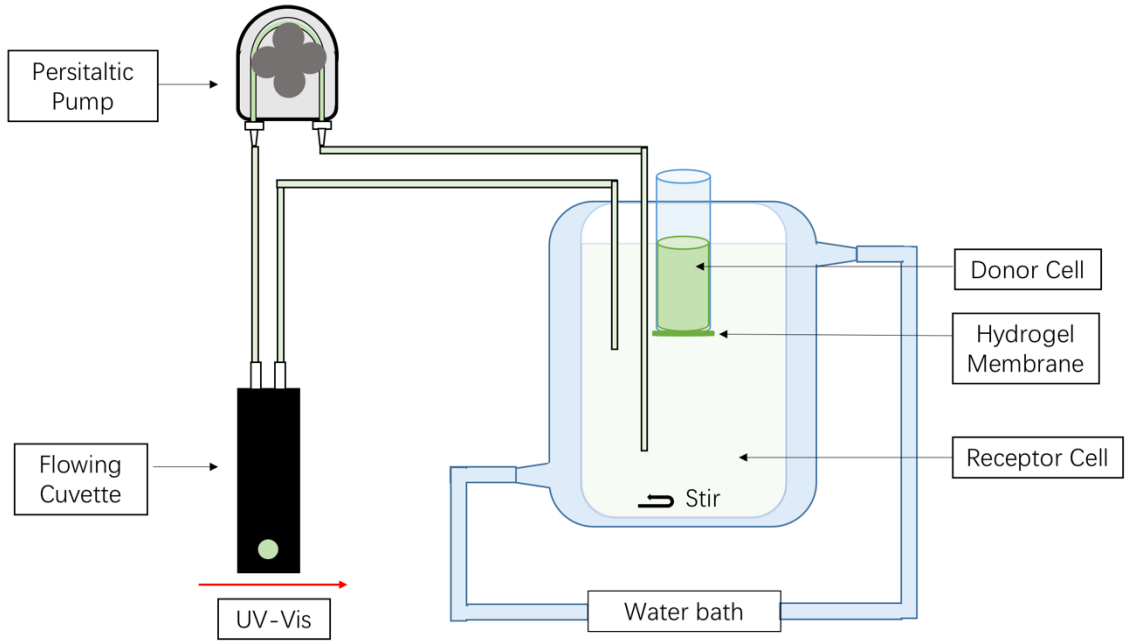

Figure 3.5 Prototype for poly(NIPA-co-MAA) permeability studies.

The setup for measure permeability of molecule through the hydrogel is illustrated in Figure 3.5. LGB was the test solute for the permeability studies. The hydrogel membrane disk was first stored at pH 4 for 12 hours to achieve equilibrium in the shrunken state. Then the hydrogel was glued to the mouth of a centrifuge tube (diameter 1.5cm), which was cut on the other end to form a cylindrical tube. The tube was submerged in a DI water tank overnight to swell the hydrogel. Before the permeability studies, a tube with the sealed hydrogel membrane was submerged in pH 7 buffer outside the tube and filled by pH 5.5 buffer for 4 hours to establish a pH gradient. A 37^{o}C water jacket beaker was used to control temperature. At the beginning of the test, 12mg model drug in 3ml pH 5.5 buffer was introduced into donor cell. The buffer in donor cell was changed each hour, which had a different pH but the same concentration of model drug. The receptor cell contained 150ml drug-free pH 7 phosphate buffer. The receptor cell was magnetically

stirred at 200rpm. Fresh drug-free phosphate buffer (pH 7) was renewed every hour. Receptor drug solution was passed through a UV-Vis spectrophotometer cuvette and returned to the receptor at the rate of 1ml/min. The absorbance of LGB was determined at 633nm.

Before the permeability studies, a tube with the sealed membrane were placed in pH 7 buffer on both sides for 2 hours. Absorbance was monitored by UV-Vis in the absence of drugs. In this blank control experiment, the change in absorbance of the solution was negligible (data not shown).

3.2.6 Phase Properties

The hydrogel pieces weighing approximately 20mg were prepared by submerging in several buffers overnight. Then the peripheral solution was removed prior to running the experiment. Thermogravimetric analysis (TGA) was used before differential scanning calorimetry (DSC) to determine the decomposition weight percentage and temperature. The temperature range examined for both instruments was 20-50°C, using a rate of 2°C/min.

3.3 Results

3.3.1 Equilibrium Swelling Studies

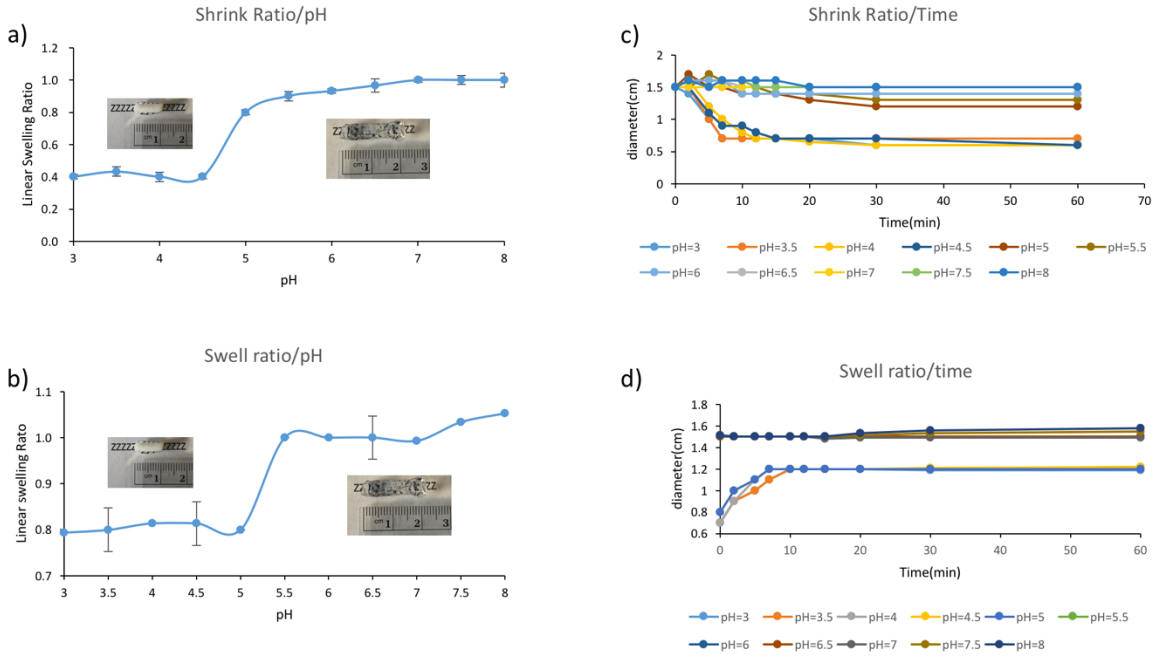

Figure 3.6 Poly(NIPA-co-MAA) linear swelling ratio with pH (a,b) and time (c,d). The shrinking and swelling ratio stands for the final diameter of hydrogel against the starting diameter for each test under respective pH.

The hydrogel in the swollen state appeared transparent, but was opaque (white) in the shrunken state. The hydrogel shrinks from the swollen state when pH dropped below 5 and the hydrogel swells from the shrunken state when pH rises above 5. The shrinking and swelling of the hydrogen took around 10 minutes to complete, regardless of pH.

3.3.2 Mechanical Properties

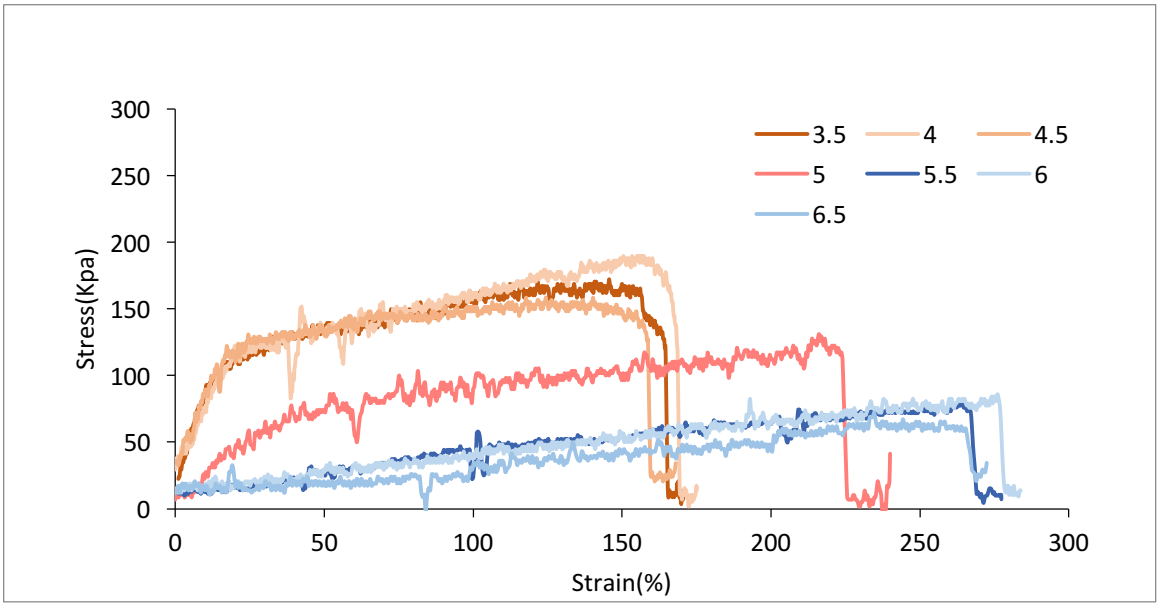

Figure 3.7 Tensile strength of the Poly (NIPA-co-MAA) hydrogel under pH 3.5 to 6.5. Strain percentage is the deformation ratio of material in continuous mechanics. Strain% = elongation /original length.

As shown in Figure 3.7, the hydrogels were highly elastic. Under pH 3.5-4.5, the hydrogel exhibited the highest mechanical strength but the lowest strain at the break point. The hydrogel under pH 5.5-6.5 shows the opposite properties, with the lowest mechanical strength and the most elongation before break. At pH = 5, the hydrogel exhibited intermediate mechanical strength and elongation at break.

3.3.3 Drug Permeability Studies

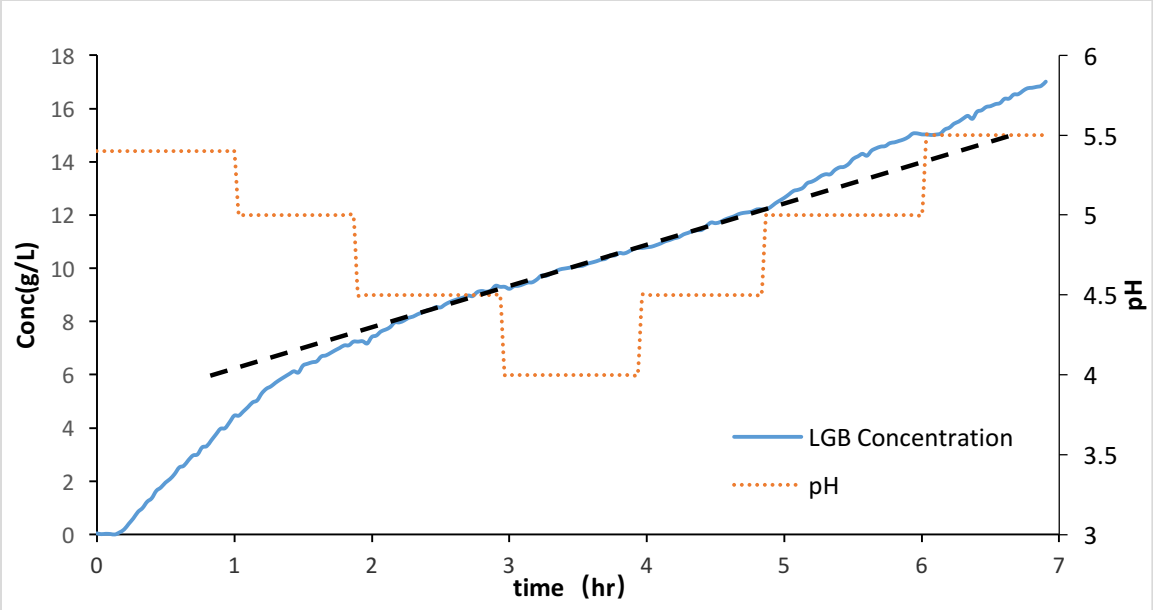

Figure 3.8 LGB permeability through the hydrogel membrane at different pH environments. Orange dashed line stands for pH in the donor cell. Blue line stands for accumulated absorbance of LGB in the receptor cell. Black dash line provides visual contrast between permeabilities in shrunken and swollen states of the hydrogel membrane.

The flux of LGB across the poly(NIPA-co-MAA) in response to a down-up staircase of pH values in the donor cell, is recorded in Figure 3.8. The absorbance of the LGB indicator was detectable at 15 minutes and remained detectable throughout seven hours. The permeation rate is quantified by the change in test solute concentration in the receptor side as a function of times. The LGB permeated through the hydrogel most rapidly during the first two hours when pH was between 5.0 and 5.5. When the pH was decreased from 5.0 to 4.5, the permeation become slower. However, the permeation increased when the pH was increased from 4.5 to 5.0. The nonlinear parts of the permeability curve are due to lag in the membrane shrinkage and swelling time.

3.3.4 Phase Properties

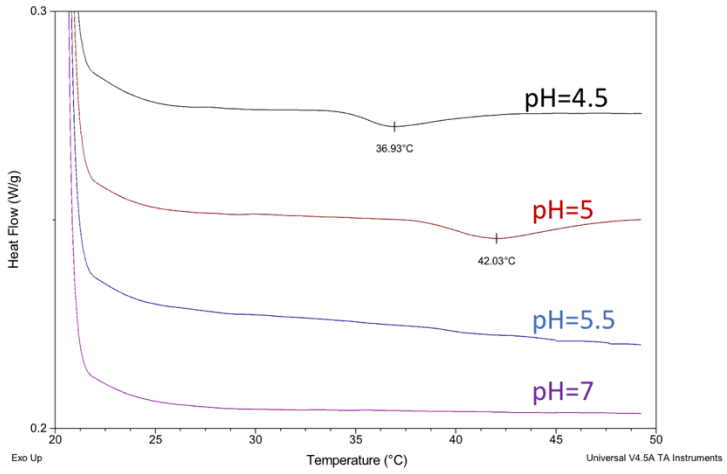

Figure 3.9 Heat flow of poly(NIPA-co-MAA) under different pH environments. To minimize the effect of water evaporation on the heat flow, the temperature was limited to 50 ^{o}C.

Thermal phase properties of the poly(NIPA-co-MAA) hydrogels are shown in figure 3.9. The curves for pH 4.5 and 5 show an endotherm during temperature increase. At the temperature where the energy absorption occurred, water likely separates from the polymer, leading to two phases corresponding to LCST behavior.

The poly(NIPA-co-MAA) hydrogel showed an LCST at 36.9^{o}C after pH = 4.5, and an LCST at 42^{o}C for pH = 5 as indicated by the obvious valleys. When pH = 5.5, there was no obvious critical temperature but the heat flow curve diminished gradually. There was no obvious phase transition when pH=7. The results suggest that at 37^{o}C, physiological temperature, hydrogel is in the shrunken state under pH = 4.5 and in swollen state under pH = 5. For hydrogel in pH 5.5 buffer, there was no obvious LCST curve shows even when the range was extended to 90^{o}C.

3.4 Discussion

3.4.1 Equilibrium Swelling Studies

As expected, hydrogels swelled at higher pH and shrink at lower pH values. However, as can be noted from Figure 3.6 a) and 3.6 b), there was a pH shift in the transition region depending on whether the hydrogel began in the swollen versus the shrunken state. This observation is indicative of hysteresis in swelling with respect to pH. Such hysteresis is a desirable property when the hydrogel membrane is included in the oscillator, described in chapter 4. It is also remarkable that, swelling or shrinking equilibrium were achieved typically within 10 minutes, which is also desirable with respect to the proposed oscillator.

3.4.2 Mechanical properties

In the study, hydrogels containing Laponite clay were used due to their reported superior mechanical properties, compared to conventional organically crosslinked hydrogels. Robust mechanical properties are needed, since in an oscillator, the hydrogel must undergo repetitive cycles of swelling and shrinking, without membrane breakage. It was found that the swollen state (high pH) is weaker but had a higher strain at the break point than the shrunken state (low pH).

3.4.3 Drug Permeability Studies

The permeability study was carried out to facilitate the prediction of the drug release through hydrogel under various pHs. We expected high permeability under high pH conditions when the hydrogels swell and much lower permeability under low pH conditions when the hydrogel is shrunken. The release profile we expected is the

hydrogel have high permeability in swollen state but completely impermeable in shrunken state. Although the slope of release profile (Figure 3.8) changed with pH, the difference was less than anticipated.

Interestingly, the LGB permeated at the highest rate during the first hour when the pH dropped from 5.5 to 5. Between 5 and 7 hours, the slope of LGB accumulation appears less steep than the first 2 hours, even though the pH remains in the same range. One explanation could be the buffering effect near the top and bottom sides of the hydrogel membrane. More specifically, the ion exchange near both sides of the membrane may influence the local pH environment and potentially affect the measured permeability of LGB. The microenvironment around membrane is difficult to determine, especially the hydrogel ion concentration.

3.4.4 Phase properties

Hydrogel consist of poly(NIPA) are known to exhibit LCST behavior in water. They swell for temperatures at and below 32^{o}C and shrink above that temperature. By adding MAA to the hydrogel chains, the poly(NIPA-co-MAA) hydrogel's LCST also becomes pH dependent, as was shown in our DSC experiment (Figure 3.9). Therefore, if the temperature is fixed at 37^{o}C, the hydrogel will be above LCST at pH 4.5 but below LCST at pH 5, hence shrunken at pH 4.5 but swollen at pH 5.

Chapter 4 Rhythmic Delivery System

4.1 Introduction

A delivery system that provides rhythmic release of hormones, powered by constant glucose concentration was developed [13-15]; however, there are several shortcomings with room for improvement.

First, marble plays a critical role, but due to the low membrane surface to chamber volume ratio, it takes a long time for hydrogen ion to exit cell II and diffuse out of the hydrogel membrane. Marble acts to eliminate the hydrogen ions produced by glucose and thereby increases the rate of the pH changes. The collapse and swelling behavior at different pH values in this system exhibits bi-stability property and hysteresis, which is active in promoting oscillations. Marble also promotes oscillations, and in its absence, the membrane may be trapped in an intermediate permeability state. Here, there is a steady state balance of glucose influx, enzymatic conversion and hydrogen clearance, and no oscillations occur in the pH of Cell II.

The current system also has a significant drawback in maintaining a regular drug release cycle through the pH oscillations. As the marble neutralizes the protons generated by glucose metabolism, its surface area decreases, and consequently the rate of proton removal and associated pH oscillations in Cell II are slowed. The accumulation of the byproduct $CaCl_2$ from the marble also correlates with slowing of the oscillation cycle. In addition, the surface area of the marble, which is a critical parameter in determining oscillating behavior [14], will slowly decrease and eventually the marble is depleted.

Moreover, for an implantable release system, additional restrictive factors need to be considered. First, the size of the device, 80ml fluid (Cell II) wrapped in a 400 μm-thick membrane, is simply too large to implant into the central nervous system. Second, the glucose-driven oscillation is unrealistic in a physiological environment. The "outside physiological" glucose concentration was optimized at 50 mM, which is 7 to 12 times the actual human glucose level (4-7mM). Additionally, the marble contributes too much mass to the drug delivery system. Moreover, the integrity of the hydrogel membrane may not be maintained, when in contact with the rough and uneven surface of the marble.

In order to transform the original system into a more practical device amenable for use *in vivo*, we reduced the Cell II volume size and removed the marble. We assume the hydrogen ions in the membrane diffuse into Cell I and are replaced by the remaining H^+ in Cell II causing pH in Cell II revert. To increase the hydrogen ion (i.e. pH) dynamics in Cell II and the membrane swell/shrink rhythmic changes in the membrane, we increase the ratio of the membrane area to volume of Cell II [16].

4.2 Materials and Methods

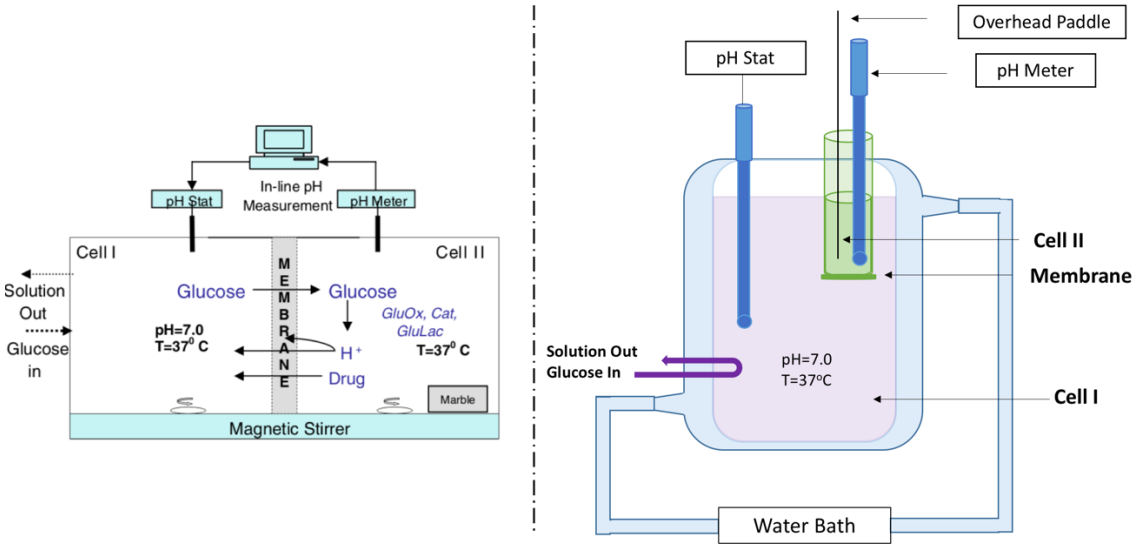

Figure 4.1 New prototype for implantable hormone release system. a) old horizontal prototype [14]. b) New vertical prototype. The self-assembled pH stat from Chapter 1 is connected with Cell I which mimics the physiological environment. Enzyme mixture colored by green in Cell II. Cell II is bathed in the solution in Cell I and is connected with Cell I only through the hydrogel layer at the bottom of the tube. Purple part exhibits circulating fresh glucose media in Cell I.

The experimental setup of the new prototype is a vertical transport cell as shown in Figure 4.1. To prime the system, 3mL of glucose-free pH 4.4 HCL buffer was added into Cell II to maintain the shrunken state of the hydrogel. Meanwhile, glucose-free 50mM saline of pH 7.0 was placed into Cell I, whose volume was 150ml. The 1.77 cm^2 (diameter 1.5cm) circular semipermeable hydrogel, poly(NIPA-co-MAA) presented in Chapter 3, was exposed to both cells. The hydrogel membrane separating Cell I and Cell II was secured on the centrifuge tube (Cell II) by sealing glue (Gorilla) and sealed by parafilm to avoid any leakage and contamination. Priming of the system took place for 3 hours. The pH gradient environment stability was maintained by pH stat in Cell I. Cell II was stirred by an overhead paddle and Cell I was mixed by a magnetic stirrer (200rpm).

After the pH gradient stabilized, various concentrations of glucose in 50mM saline were recirculated with Cell I at 1ml/min by a peristaltic pump. Fresh pH=4.4 enzyme solution, glucose oxidase from aspergillus niger (Sigma 225970U/mg) and catalase (Sigma 7741IU/mg), with trace amounts of gluconolactonase) replaced the buffer solution in Cell II. Thereafter, two pH meters recorded data every one minute in Cell I and Cell II. Meanwhile, the pH stat designed in Chapter 1 maintained the pH in Cell I at pH 7.0.

Due to the high cost of GnRH, we did not accurately track the drug release profile. The drug release condition is reflected by the pH inside Cell II and membrane swelling state, which is showed in Chapter 2. More specifically for drug rhythmic delivery in this system, when the pH higher than 5 in chamber II, the membrane is in a swollen state and the cumulative drug release is fast. Conversely, at pH less than 5, drug release is slow due to the collapsed state of the membrane.

4.3 Results

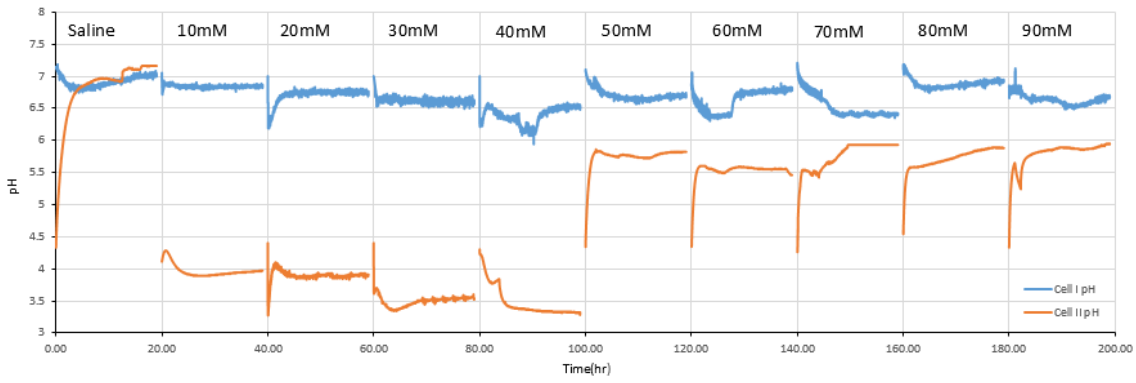

Figure 4.2 Ten independent oscillation experiments with various glucose concentration in Cell I.

Figure 4.2 depicts the pH as a function of time for ten separate 20-hour pH recordings in the pulsatile drug delivery system. pH oscillations were not observed under any glucose

concentration. The saline control aimed to establishes the rate of hydrogen ion release from the membrane at Cell II. The graph shows that the hydrogen ion transports through the hydrogel membrane in less than two hours. With different glucose concentrations in Cell II, each run shows constant intermediate pH by the influence of glucose concentration from 0-40mM. At higher glucose concentrations in this range for Cell II, the pH decreased. Once the concentration of glucose reached 50mM and higher, the pH value of Cell II stabilized around 5.5-6, regardless glucose concentrations. In all cases, the Cell I pH was maintained around 6.5-7 by the pH-stat.

4.4 Discussion

Our Study was unable to show pH oscillations in Cell II as proposed under the various glucose concentration environments as proposed. Our finding is not consistent with the theoretical predictions reported in the literature [16]. The previous study theorized that the hydrogel membrane would act as a semipermeable barrier to allow glucose transport when swollen (pH > 5) and block glucose transport when shrunken (pH < 5). Once glucose from the physiological environment (Cell I) enters the implantable device (Cell II), it will be converted by enzymes to produce hydrogen ions. Then, the hydrogen ions are expected to lower the pH in Cell II and be attracted to the negatively charged hydrogen membrane to transform it from being swollen to shrunken. As a result, the entry of glucose to Cell II is temporarily blocked by the shrunken hydrogel. The hydrogel will become permeable again once hydrogen ion in Cell II crossed the membrane to Cell I where pH is regulated by pH stat. The pH oscillation in Cell II would take place when all the steps are fulfilled as described. However, this sequence of events was not observed in our system.

At this point, we believe that theoretical approach is sound, and the experimental failure arose from inappropriate assumptions. Because more than one variable was changed to optimize the system for *in vivo* use, it is not possible to determine which experimental parameter is the root cause or even if there are more than one parameter giving rise to the failure. As such, there is a need to back track and take a systematic, step by step approach.

Specifically, the same oscillation patterns in the original setup must be reproduced [14], in which the home designed pH-stat for the commercial autotitrator introduced in Chapter 2 is used. With success, the second step would be to replace the organically crosslinked poly(NIPA-co-MAA) membrane with our laponite-crosslinked membrane, still using the original setup. This systematic approach could reveal the problems, without introducing extra variables such as volume of Cell I, surface area of the membrane, and the removal of marble from the system.

Chapter 5 Conclusions and Future Directions

5.1 Conclusions

We successfully programmed the pH stat able to perform well for the project. The poly (NIPA-co-MAA) hydrogel's swelling ratio, mechanical strength, permeability and phase properties were characterized. A new prototype of the GnRH rhythmic delivery system was examined, but did not function as required.

5.1.1 pH Stat

The self-assemble pH stat is economical and easy to control. The pH controller is suitable for most titration conditions with model and hardware adjustment. The peristaltic pumps are adaptable for accurate dosing applications with a variety of tube size and pump ratios available. The theoretical acid-base equilibrium equation-based program is applicable to any titration program; however, the empirical model-based program provides more rapid response.

5.1.2 pH-Sensitive Hydrogel

The 100 μm nanoclay cross-linked poly (NIPA-co-MAA) was synthesized successfully. The equilibrium swelling ratio, mechanical properties, drug permeability under various pH environment and phase properties were presented. The equilibrium swelling studies provided guidance for the measurable permeability variations over a range of pH value. The mechanical studies showed that the hydrogel was strongest in the shrunken state. The phase properties reflect LCST behavior. The permeability provided the pH drug release profiles, which did not vary to the extent required for a pulsatile system.

5.1.3 Rhythmic Delivery System

The new prototype for the implantable pH-oscillator rhythmic hormone release system was assembled but did not produce the intended pH oscillations. Various glucose concentrations for oscillation experiments were attempted, but they all result in a constant, steady state pH behavior.

5.2 Future Directions

5.2.1 pH-Stat

The peristaltic pump and tubing hardware are easy to adjust for high customizability. Beyond that, for future more precise titrations, more data can be obtained by manual titration, and better calibration curves can be determined.

5.2.2 pH-Sensitive Hydrogel

A therapeutic system which can resist abrasion in the target organ or site is required. Poly(NIPA-co-MAA) crosslinked by acylated allylic starch could be used to replace of the nanoclay-crosslinked hydrogels. The high tensile properties and swelling ratio have demonstrated for such system [41]. In addition, the potential complication due to the ionized nanoclay particles would be eliminated in the starch-crosslinked system [36].

5.2.3 Rhythmic Delivery System

As a future step in constructing a pulsatile delivery system, the enzyme could be entrapped or be covalently linked into the hydrogel matrix [42]. The size of the hydrogel capsule (Cell II) can reduced, since the volume of its contents is smaller by localizing the enzymes in the hydrogel membrane. By reducing the need for glucose to cross the hydrogel membrane, this design can allow glucose molecules to be better taken up by the enzymes. Cell II will likely become more sensitive to glucose concentration, given that

the enzymes will encounter glucose molecules on the surface of the hydrogel capsule. Buffer byproducts of the glucose metabolism would diffuse away from the membrane in the shrinking process [43-45]. As a result, the pH oscillation in Cell II will be strictly regulated by glucose conversion. The previous concern of increased oscillation cycle caused by buffer buildup will likely be resolved [14]. It will be easier for plasma oxygen take part in the enzyme metabolism, and therefor we can overcome the oxygen consumption problem. Once the oscillation challenge is overcome, we shall proceed to study the drug release features of the system.

Bibliography

[1] Balasubramanian, Ravikumar, Andrew Dwyer, Stephanie B. Seminara, Nelly Pitteloud, Ursula B. Kaiser, and William F. Crowley Jr. "Human GnRH deficiency: a unique disease model to unravel the ontogeny of GnRH neurons." *Neuroendocrinology* 92, no. 2 (2010): 81-99.

[2] Balasubramanian, Ravikumar, and William F. Crowley Jr. "Isolated Gonadotropin-Releasing Hormone (GnRH) Deficiency." In GeneReviews®[Internet]. University of Washington, Seattle, 2017.

[3] Mylonas, Constantinos C., and Yonathan Zohar. "Use of GnRHa-delivery systems for the control of reproduction in fish." Reviews in fish biology and fisheries 10, no. 4 (2000): 463-491.

[4] Herbison, Allan E. "Noradrenergic regulation of cyclic GnRH secretion." Reviews of Reproduction 2, no. 1 (1997): 1-6.

[5] Iremonger, Karl J., Stephanie Constantin, Xinhuai Liu, and Allan E. Herbison. "Glutamate regulation of GnRH neuron excitability." Brain research 1364 (2010): 35-43.

[6] Bommannan, D. Bommi, Janet Tamada, Lewis Leung, and Russell O. Potts. "Effect of electroporation on transdermal lontophoretic delivery of luteinizing hormone releasing hormone (LHRH) in vitro." Pharmaceutical research 11, no. 12 (1994): 1809-1814.

[7] Bhatia, Kuljit S., Shen Gao, and Jagdish Singh. "Effect of penetration enhancers and iontophoresis on the FT-IR spectroscopy and LHRH permeability through porcine skin." Journal of controlled release 47, no. 1 (1997): 81-89.

[8] Lemay, A., and N. Faure. "Fourteen day versus twenty-one day regimens of intermittent intranasal LHRH agonist sequentially combined with an oral progestogen as anti-ovulatory contraceptive approach." J Clin Endocrinol Metab 63 (1986): 1379.

[9]Satarkar, Nitin S., and J. Zach Hilt. "Magnetic hydrogel nanocomposites for remote controlled pulsatile drug release." Journal of Controlled Release 130, no. 3 (2008): 246-251.

[10] Kikuchi, Akihiko, Minako Kawabuchi, Masayasu Sugihara, Yasuhisa Sakurai, and Teruo Okano. "Pulsed dextran release from calcium-alginate gel beads." Journal of Controlled Release 47, no. 1 (1997): 21-29.

[11] Roy, Pallab, and Aliasgar Shahiwala. "Multiparticulate formulation approach to pulsatile drug delivery: current perspectives." Journal of controlled release 134, no. 2 (2009): 74-80.

[12] https://www.mayoclinic.org/diseases-conditions/diabetes/symptoms-causes/syc-20371444

[13] Misra, Gauri P., and Ronald A. Siegel. "New mode of drug delivery: long term autonomous rhythmic hormone release across a hydrogel membrane." Journal of controlled release 81, no. 1-2 (2002): 1-6.

[14] Bhalla, Amardeep S., and Ronald A. Siegel. "Mechanistic studies of an autonomously pulsing hydrogel/enzyme system for rhythmic hormone delivery." Journal of Controlled Release196 (2014): 261-271.

[15] Mujumdar, Siddharthya K., Amardeep S. Bhalla, and Ronald A. Siegel. "Novel hydrogels for rhythmic pulsatile drug delivery." In Macromolecular symposia, vol. 254, no. 1, pp. 338-344. Weinheim: WILEY- VCH Verlag, 2007.

[16] Dhanarajan, Anish P., Jon Urban, and Ronald A. Siegel. "A model for a hydrogel-enzyme chemomechanical oscillator." 2004.

[17] https://www.graylineinc.com/whitepapers/peristaltic-pump-tubing.html

[18] https://www.mrwatt.eu/en/shop/electronics-and-domotics/electronics-and-domotics-boards/tarjeta-raspberry-pi3-model-b.html

[19]http://static6.arrow.com/aropdfconversion/4822314840f9b6e00b2d75fe5dff3b59dfc74a34/pgurl_5148356817969200.pdf

[20] http://www.scienceexposure.com/raspberry-pi/buffer-solution-ph-adjuster-raspberry-pi/

[21] https://github.com/ismailuddin/raspberrypi/blob/master/buffer-ph-adjuster/calibrate.py

[22] https://github.com/ismailuddin/raspberrypi/blob/master/buffer-ph-adjuster/buffer-ph-range.py

[23] O. Wichterle, D. Lim, Hydrophilic gels in biologic use, Nature 185 (1960) 117

[24] Lee, Kuen Yong, and David J. Mooney. "Hydrogels for tissue engineering." Chemical reviews 101, no. 7 (2001): 1869-1880.

[25] Byrne, Mark E., Kinam Park, and Nicholas A. Peppas. "Molecular imprinting within hydrogels." Advanced drug delivery reviews 54, no. 1 (2002): 149-161.

[26] Kamoun, Elbadawy A., El-Refaie S. Kenawy, and Xin Chen. "A review on polymeric hydrogel membranes for wound dressing applications: PVA-based hydrogel dressings." Journal of advanced research 8, no. 3 (2017): 217-233.

[27] Toussaint, J. F., A. Dubois, M. Dispas, D. Paquet, C. Letellier, and P. Kerkhofs. "Delivery of DNA vaccines by agarose hydrogel implants facilitates genetic immunization in cattle." Vaccine 25, no. 7 (2007): 1167-1174.

[28] Qiu, Yong, and Kinam Park. "Environment-sensitive hydrogels for drug delivery." Advanced drug delivery reviews 53, no. 3 (2001): 321-339.

[29] Shim, Woo Sun, Jae Sun Yoo, You Han Bae, and Doo Sung Lee. "Novel injectable pH and temperature sensitive block copolymer hydrogel." Biomacromolecules 6, no. 6 (2005): 2930-2934.

[30] Shim, Woo Sun, Jae Sun Yoo, You Han Bae, and Doo Sung Lee. "Novel injectable pH and temperature sensitive block copolymer hydrogel." Biomacromolecules 6, no. 6 (2005): 2930-2934.

[31] Gupta, Piyush, Kavita Vermani, and Sanjay Garg. "Hydrogels: from controlled release to pH-responsive drug delivery." Drug discovery today 7, no. 10 (2002): 569-579.

[32] Zhang, Jie, Rui Xie, Shi-Bo Zhang, Chang-Jing Cheng, Xiao-Jie Ju, and Liang-Yin Chu. "Rapid pH/temperature-responsive cationic hydrogels with dual stimuli-sensitive grafted side chains." Polymer 50, no. 11 (2009): 2516-2525.

[33] Brazel, Christopher S., and Nicholas A. Peppas. "Synthesis and Characterization of Thermo-and Chemomechanically Responsive Poly (N-isopropylacrylamide-co-methacrylic acid) Hydrogels." Macromolecules 28, no. 24 (1995): 8016-8020.

[34] Shibayama, Mitsuhiro, Masato Morimoto, and Shunji Nomura. "Phase separation induced mechanical transition of poly (N-isopropylacrylamide)/water isochore gels." Macromolecules27, no. 18 (1994): 5060-5066.

[35] Ono, Yousuke, and Toshiyuki Shikata. "Hydration and dynamic behavior of poly (N-isopropylacrylamide) s in aqueous solution: a sharp phase transition at the lower critical solution temperature." Journal of the American Chemical Society 128, no. 31 (2006): 10030-10031.

[36] Mujumdar, Siddharthya K., and Ronald A. Siegel. "Introduction of pH- sensitivity into mechanically strong nanoclay composite hydrogels based on N-isopropylacrylamide." Journal of Polymer Science Part A: Polymer Chemistry 46, no. 19 (2008): 6630-6640.

[37] Siegel, Ronald A., Eric E. Nuxoll, Marc A. Hillmyer, and Babak Ziaie. "Top-down and bottom-up fabrication techniques for hydrogel based sensing and hormone delivery microdevices." In 2009 Annual International Conference of the IEEE Engineering in Medicine and Biology Society, pp. 232-235. IEEE, 2009.

[38] Haraguchi, K., Li, H.J., Matsuda, K., Takehisa, T. and Elliott, E., 2005. Mechanism of forming organic/inorganic network structures during in-situ free-radical polymerization in PNIPA− clay nanocomposite hydrogels. Macromolecules, 38(8), pp.3482-3490.

[39] Xiang, Yuanqing, Zhiqin Peng, and Dajun Chen. "A new polymer/clay nano-composite hydrogel with improved response rate and tensile mechanical properties." European Polymer Journal 42, no. 9 (2006): 2125-2132.

[40] Haraguchi, Kazutoshi, Toru Takehisa, and Simon Fan. "Effects of clay content on the properties of nanocomposite hydrogels composed of poly (N-isopropylacrylamide) and clay." Macromolecules 35, no. 27 (2002): 10162-10171.

[41] Tan, Ying, Kun Xu, Pixin Wang, Wenbo Li, Shumiao Sun, and LiSong Dong. "High mechanical strength and rapid response rate of poly (N-isopropyl acrylamide) hydrogel crosslinked by starch-based nanospheres." Soft Matter 6, no. 7 (2010): 1467-1471.

[42] Sheldon, Roger A. "Enzyme immobilization: the quest for optimum performance." Advanced Synthesis & Catalysis 349, no. 8- 9 (2007): 1289-1307.

[43] Bao, Jie, Keiji Furumoto, Makoto Yoshimoto, Kimitoshi Fukunaga, and Katsumi Nakao. "Competitive inhibition by hydrogen peroxide produced in glucose oxidation catalyzed by glucose oxidase." Biochemical engineering journal 13, no. 1 (2003): 69-72.

[44] Harris, James M., Catherine Reyes, and Gabriel P. Lopez. "Common causes of glucose oxidase instability in in vivo biosensing: a brief review." Journal of diabetes science and technology 7, no. 4 (2013): 1030-1038.

[45] Zia, Muhammad Anjum, Muhammad K. Saeed Khalil-ur-Rahman, Fozia Andaleeb, Muhammad I. Rajoka, Munir A. Sheikh, Iftikhar A. Khan, and Azeem I. Khan. "Thermal characterization of purified glucose oxidase from a newly isolated Aspergillus niger UAF-1." Journal of clinical biochemistry and nutrition 41, no. 2 (2007): 132.